ANALYSIS OF hTHY28 EXPRESSION IN HELA CELLS

by

MICHAELLE PURDEE

(Under the Direction of Mark M.Compton)

ABSTRACT

The hThy28 gene was isolated from the human cervical carcinoma cell line, HeLa, and its expression was analyzed in these cells. Structural motif analysis reveals that hThy28 is a 225 amino acid protein that contains potential phosphorylation sites, a myristolation site, an amidation site, a glycosolation site, a sumoylation site, a DUF589 motif, and a nuclear localization site. Transfection of hThy28/Enhanced Green Fluorescent Protein constructs into HeLa cells revealed intense fluorescence in the nuclear localization of this gene product. Functional analysis of hThy28 was investigated using RNA interference methodology. These studies suggest that this gene may protect cells from undergoing apoptosis since hThy28 gene silencing promotes cell death in the presence of apoptotic mediators. Future work will focus on the role of hThy28 in the apoptotic pathway.

INDEX WORDS: Apoptosis, RNA interference, Thy28, HeLa cells, Enhanced Green Fluorescent Protein

ANALYSIS OF hTHY28 EXPRESSION IN HELA CELLS

by

MICHAELLE PURDEE

B.S, The University of Georgia, 2002

A Thesis Submitted to the Graduate Faculty of The University of Georgia in Partial Fulfillment

of the Requirements for the Degree

MASTER OF SCIENCE

ATHENS, GEORGIA

2006

ANALYSIS OF hTHY28 EXPRESSION IN HELA CELLS

by

MICHAELLE PURDEE

Major Professor: Mark Compton

Committee: Adam Davis
Amy Batal

Electronic Version Approved:

Maureen Grasso
Dean of the Graduate School
The University of Georgia
August 2006

TABLE OF CONTENTS

LIST OF TABLES

Page

LIST OF FIGURES

Page

CHAPTER 1

INTRODUCTION

Apoptosis

In multicellular organisms, complex networks of signaling systems are required to regulate physiological processes that alter cellular function, including cell to cell communication, cell proliferation, and cell differentiation. One important signaling pathway is demonstrated by the cell's use of the apoptotic cell death pathway.

Apoptosis is a Greek term coined by Kerr and associates [1] that refers to the "falling of leaves" from a tree. His work, as well as that of other investigators [2-5], has focused on the importance of apoptosis in maintaining the balance between cell proliferation and cell deletion, where apoptosis appears to be the most common form of cell death [1, 6, 7]. Peter Krammer and his associates were among the first investigators to publish work related to the signaling systems involved in apoptosis. Their work indicates that apoptosis plays important roles in "embryogenesis, metamorphosis, tissue atrophy, and tumor regression" [7]. Apoptosis is also important in the immune protection against viral infections. Cells can invoke a type of "defensive cellular suicide", where the killing of the infected cells occurs prior to the spread of the virus to other cells. Furthermore, when a cell recognizes that it has been infected with a virus, it activates pathways that lead to the presentation of the viral antigen on the cell membrane. The viral protein is bound to the Major Histocompatability Complex (MHC) and relocates to the outer membrane of the cell where it exposes the antigen signal to cytotoxic T lymphocytes and natural killer cells. In turn, these cells recognize this antigen signal as being foreign and kill the infected cell [3, 4]. Antigen presentation also activates T and B-lymphocytes which proliferate

and differentiate to generate an immune response that eliminates the threat. Once the threat is no longer present there is a need to reduce the immune response. In response to this need, apoptotic pathways are activated to down regulate the amplified immune response after the foreign threat has passed. The continued presence of an elevated number of lymphocytes can result in autoimmune diseases, immunodeficiency, and lymphoid malignancies, further supporting the physiological importance of apoptosis [8].

Apoptosis and its normal signaling pathways have come under intense study to better understand the diseases that are caused by its disregulation. Some examples of the diseases that have been studied include acquired immunodeficiency syndrome, neurodegenerative disorders, and cancer [9]. Tumor suppressor genes appear to be intimately involved in these disease processes. Over twenty tumor suppressor genes have been discovered and all of these genes appear to play an important role in cancer development. These genes are defined as "genes whose loss of function promotes malignancy" [10]. The products of tumor suppressor genes affect growth, regulation, differentiation, and apoptosis and thereby inhibit the transformation of a normal cell to a tumor cell. Genetic lesions in the cellular DNA activate tumor suppressor gene products that promote cellular deletion and prevent the transformation of a normal cell into a malignant cell. This is an important process in cancer prevention as the potential for malignant transformation of cells, into tumor cells, is removed along with the removal of genetic faults. On the other hand, mutations that inactivate tumor suppressor gene function promote the neoplastic transformation of cells. [10, 11]

Apoptosis Morphology as Compared to Necrosis

Apoptosis is a type of programmed cell death that is different from cellular death caused by necrosis. Necrosis, which is also referred to as accidental cell death, is usually caused by extreme trauma or injury to the cell. Swelling of the cell, which leads to rupture, and lysis of the cell membrane is characteristic of necrosis. When the cell ruptures, its contents are released into the extra cellular space causing an inflammatory response that causes injury or death to adjacent cells, which can lead to further tissue damage [12]. On the other hand, cellular shrinkage, "blebbing" of the cell membrane, chromatin condensation, and DNA fragmentation characterize a cell undergoing apoptosis. During apoptosis, cellular lamins and actin-cytoskelton elements are cleaved. This cleavage removes the cell's structural support, which in turn, causes the cellular and nuclear membranes to loose their shape and form the characteristic blebbing morphology. The membrane transformation is associated with the relocation of phosphatidylserine to the outer membrane leaflet. This extracellular exposure of phosphatidyl serine is believed to activate cellular phagocytosis by adjacent cells or macrophages. The chromatin condensation associated with apoptosis is mediated by the internucleosomal cleavage of DNA into multiples of approximately 180 base pairs. Generation of nucleosomal DNA fragments is the end product of an activated endonuclease, CAD (Caspase-Activated DNase). CAD, is normally found inactive in the cytosol of cells, however, during apoptosis it is activated via caspase proteinase and translocates into the nucleus where it cleaves the DNA. Collectively, these processes generate a membrane-bound apoptotic body that is easily phagocytosed by neighboring cells or macrophages. Thus, apoptotic body formation prevents the loss of cellular contents into the interstitial space and the induction of the inflammatory response which are characteristics of necrosis. [12, 13]

Extrinsic Apoptotic Pathways

The receptor-mediated pathways, or extrinsic pathways of apoptosis induction and signaling, are initiated by the binding of specific ligands with death receptors located on the surface of target cells (Figure 1). This ligand/receptor complex triggers a series of events that leads to the induction of apoptosis inside the cell. Death receptors are type I membrane proteins (proteins with a single α-helical trans-membrane domain where the amino terminus is presented on the cell's surface and the carboxyl terminus is located within the cell) that are part of the Tumor Necrosis Factor (TNF) receptor superfamily. The five known death receptor families are: TNF-R1, CD95/Fas/APO-1, TRAMP/DR3/WSL/LARD, TRAIL-R1/DR4/APO-2, and TRAIL-R2/DR5. Their known ligands are TNF, CD95L, lymphotoxin-α (LTα), and TRAIL respectively. These ligands are type II transmembrane proteins (protein with a single α-helical trans-membrane domain where the carboxyl terminus is found on the extracellular surface and the amino terminus is found in the interior of the cell membrane), with the exception of LTα, that contains three identical subunits which activate their receptors by oligomerization [2]. The death receptors are characterized by an intracellular death domain that is approximately 80 amino acids long. This death domain is highly homologous among death receptors. The extracellular components of the receptors contain at least 2-6 cysteine-rich domains. These domains are approximately 40 amino acid long imperfect repeats with about 6 cysteine residues in each domain [2].

Although many different pathways have been described that induce apoptosis, the well characterized Fas signaling pathway is used as an example here (Figure 1). Fas/Apo-1/CD95 is a 317 amino acid type I transmembrane glycoprotein with three extra cellular, cysteine-rich domains (CRDs). Fas is a member of the nerve-growth-factor receptor family, and the CRDs that

form this cell surface death receptor characterize it as part of the tumor necrosis factor (TNF) super family [12, 14, 15]. The Fas apoptotic signaling cascade is activated when Fas-ligand (FasL) binds to the receptor or when the receptor becomes cross-linked by agonistic anti-Fas antibodies [16]. The FasL exists as a single, soluble death ligand or as a membrane bound death ligand, which is usually found on the surface of activated lymphocytes and natural killer cells [15].

The Fas receptor forms a homo-trimer with the cysteine-rich domains CRD2 and CRD3. This trimer makes up the major contact surfaces for one FasL to bind to the receptors on the extracellular surface. The globular protein interaction domain found on the cytoplasmic portion of Fas, known as the death domain, rapidly recruits and interacts with the adaptor molecule FADD (Fas-associated Death Domain protein)/Mort-1 when FasL binds to the receptor [8, 14, 15]. FADD has two protein interaction domains, the death domain (DD) and the death effector domain (DED). The DD of FADD binds to the C-terminal portion of the Fas DD after recruitment. Then the FADD DED on the N-Terminal portion of the molecule recruits and binds to other molecules that contain a DED. An example of an apoptotic mediator that contains a DED is pro-caspase-8; when it binds to the DED of FADD it forms a complex called the Death Inducing Signaling Complex or DISC (see Figure 1) [15, 17]. The two protein domains, DD and DED, of FADD function independently of each other and are only capable of undergoing homodimerization. This restriction refers to the fact that a death domain of FADD will not interact with the death effector domain of another molecule and vice versa [15]. In other word DD will only dimerize with other DD and DEDs will only dimerize with other DEDs.

Soluble FasL is not as potent an apoptotic death signal as membrane bound FasL. This is because a single FasL binds to the trimeric Fas receptor which engages only one pro-caspase-8 to

bind to form the DISC [8]. Pro-caspase-8 must dimerize with itself to undergo auto-cleavage to achieve its active form. If another FasL links with the previous FasL then another trimeric Fas is recruited. This allows for another pro-caspase-8 to bind into the DISC and apoptosis can be initiated. Apoptosis requires at least two ligands binding to two trimeric receptors, forming an oligomerization of the receptors, to be initiated. Membrane bound FasLs are found in large numbers on the surface of lymphocytes making oligomerization of Fas receptors more frequent. The apoptotic response is increased when greater concentrations of FasL are found. Likewise, greater concentrations of soluable FasL increase FasL receptor bound cross-linking, which increases the apoptotic response. [15, 17]

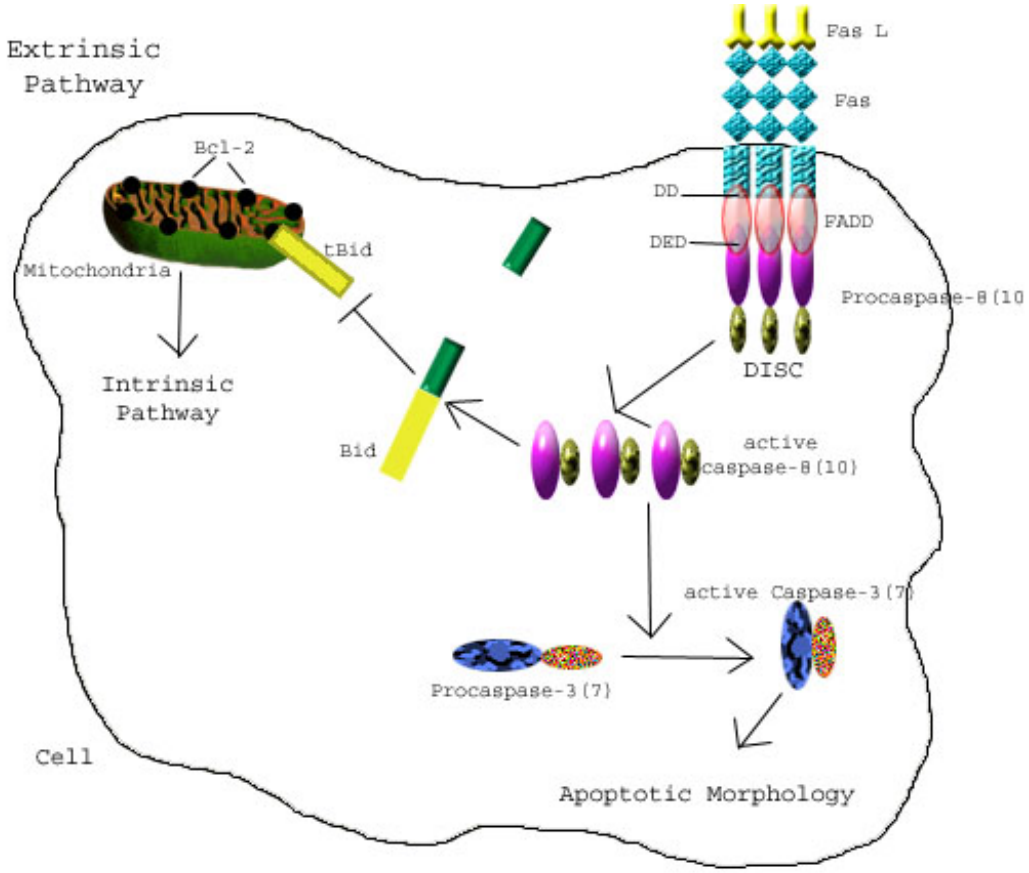

Figure 1: Extrinsic Pathway of Apoptosis The Fas death ligands bind onto the extracellular portions of the membrane bound receptor, Fas. This induces a conformational change in the intracellular domain of the receptors. This new conformation allows an adaptor protein, FADD, to bind. FADD then recruits a specific class of proteins called caspases, in this example procaspase-8(10). This configuration allows for the procaspases to autoproteolytically cleave each other, rendering them active and free to move into the cytoplasm of the cell. These active caspases, in turn, activate other caspases, such as caspase-3(7), to initiate the apoptotic morphology. This pathway can also initiate the intrinsic pathway when caspases-8(10) cleave the pro-apoptotic agent Bid allowing the truncated form of tBid to disrupt the mitochondrial transmembrane potential.

Intrinsic Apoptotic Pathways

Apoptosis can be initiated and controlled by the mitochondria independently from death receptors (Figure 2). The mitochondrial transmembrane potential ($\Delta\Psi_m$), the electrical potential held between the inner and outer mitochondrial membrane, appears to play a pivotal role in this process. The inner mitochondrial membrane creates the transmembrane potential because it is quasi-impermeable to small molecules [18]. Mitochondrial function is dependent upon this membrane potential to generate ATP. Unfavorable metabolic conditions can cause a reduction of the mitochondrial transmembrane potential and initiate apoptosis. Such conditions include growth factor withdrawal, genotoxic stress, detachment of adherent cells (anoikis), reactive oxygen species, ionizing radiation, chemotherapeutic drugs, cellular depletion of glutathione, depletion of $NADPH_2$, depletion of ADP/ATP, or supraphysiological levels of cytosolic Ca^{2+} [18-20]. This reduction in membrane potential is thought to be due to the opening of the mitochondrial permeability transition (PT) pore. Along with the reduction in transmembrane potential, an increase in the mitochondrial matrix volume and mechanical disruption of the outer mitochondrial membrane occurs.

The Bcl-2 family of proteins regulates the integrity of the mitochondrial membrane. This family of proteins can be divided into three different groups, the anti-apoptotic group, the BH3-only proteins, and the pro-apoptotic group. The anti-apoptotic members that include Bcl-2 and Bcl-$X_{L,}$ are associated with the outer mitochondrial membrane. These gene products maintain the integrity of the mitochondrial membranes by enhancing the export of H+ ions from the inter-mitochondrial space [21]. The Bcl-2-homology domain 3 (BH3-only) proteins, such as Bid, are inactive proteins that are associated with organelles, such as the mitochondria. When activated they affect the third group, the pro-apoptotic members, also found in the cytosol, examples of

which include Bax, Bak, and Bok [20, 21]. When the pro-apoptotic members are activated they complex with the anti-apoptotic members,Bcl-2 or Bcl-$X_{L,}$ forming a heterodimer that inhibits their function. Although the exact mechanisms of this interaction are unknown, the over all affect is a loss of function in the electron transport chain and a resulting loss of mitochondrial function. This disruption causes the outer mitochondrial membrane to become permeabilized and thus allows the release of inner mitochondrial proteins into the cytosol.

When the mitochondrial membrane is disrupted, cytochrome c is released from the mitochondria. Cytochrome c is normally found in the inter-mitochondrial membrane, however, when the mitochondrial membrane is disrupted; cytochrome c enters the cytosol of the cell. Upon entry into the cytoplasmic compartment, cytochrome c binds to Apaf-1 (apoptotic protease activating factor), along with dATP and recruits pro-caspase-9 (see Figure 2) [20, 22]. Pro-caspase-9 is an initiator caspase and when combined with dATP, Apaf-1 and cytochrome c it forms the caspase-9 activator complex. Many of these complex's join to form the apoptosome. Unlike other caspases, caspase-9 does not lose its amino terminal-peptide when cleaved and activated. This enables the active caspase-9 to remain associated with the apoptosome and to activate the downstream caspases, specifically caspase-3 and -7 (see Figure 2) [16]. Activation of these downstream caspases mediates the apoptotic cell death process. In addition, Diablo/Smac are mitochondrial proteins that are released into the cytosol of the cell when the mitochondrial membrane is disrupted, as seen in Figure 2. These proteins promote apoptosis by binding to inhibitor of apoptosis (IAP) proteins which compromise the effect of caspases in the cell [23].

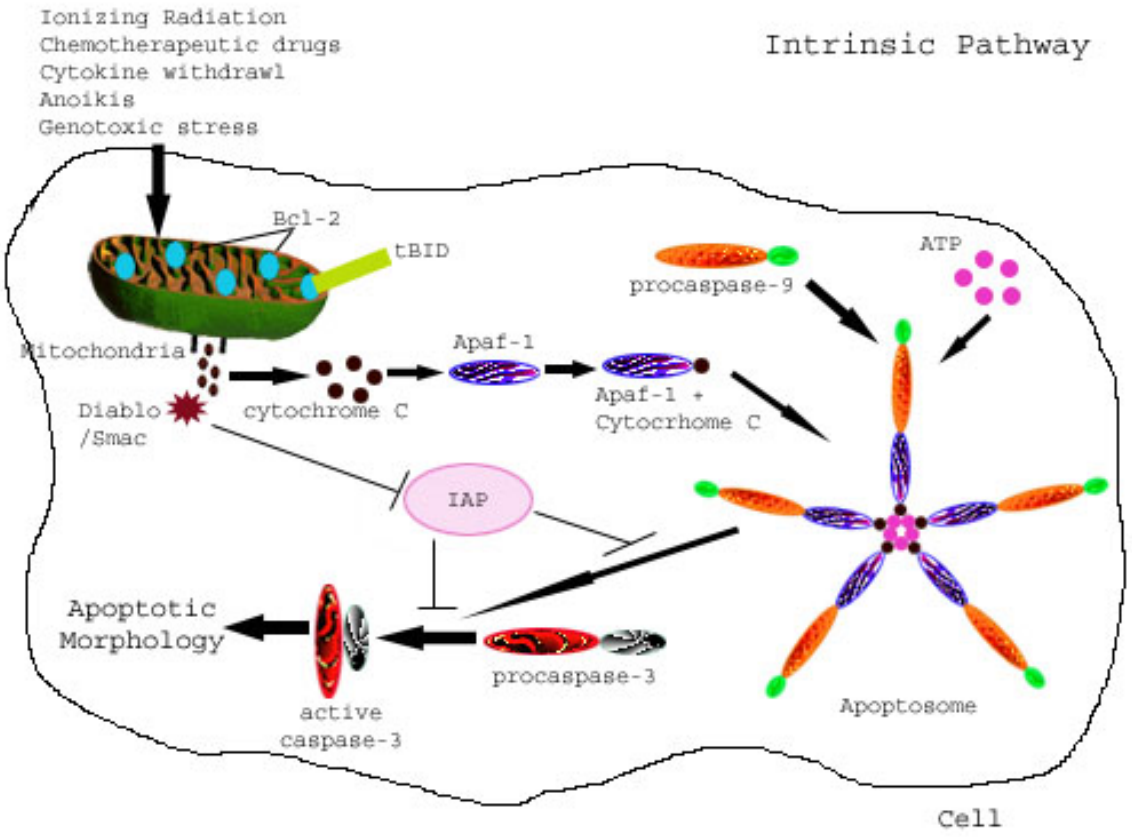

Figure 2: Intrinsic Pathway of Apoptosis The introduction of genotoxic stresses on the cell (such as ionizing radiation and chemotherapeutic drugs) ultimately leads to the disruption of the mitochondrial transmembrane potential. When this occurs, proapototic factors in the mitochondria leak out into the cytoplasm. One of these factors, cytochrome c, forms a complex with apoptotic protease activating factor (Apaf-1), and activates it. In turn, this complex recruits pro-caspase-9 and dATP to form the caspase-9 activator complex known as the apoptosome. The apoptosome then activates other cytoplasmic caspases (such as caspase-3) that mediate the characteristic morphology of apoptotic cells via their proteolytic activity. In addition, Diablo/Smac is also released into the cytoplasm from the mitochondria during the intrinsic apoptotic pathway. These gene product inhibits proteins that normally inhibit apoptosis (IAP), thereby promoting the apoptotic process.

Caspase Activation Pathways

Caspases are defined as a "family of cysteine proteases with specificity for aspartic acid residues" [24]. Caspase stands for cysteine-dependent aspartate specific protease [25]. Activation of these proteinases results in the cleavage of a wide variety of cellular proteins such as lamins,

actin-cytoskelton and other caspases. This protein cleavage simultaneously activates the apoptotic pathway by initiator caspases and destroys the cellular structure by executioner caspases [24].

All caspases are synthesized as pro-caspases or zymogens that are proteolytically inactive. The pro-caspases share a common protein structure that contains a large p10 domain and a smaller p20 catalytic subunit domain. The differences among the N-terminal pro-domains are the distinguishing features of various caspases. Two different groups of caspases can be defined based on the structure of the N-terminal pro-domain. The first group is referred to as the initiator caspases and members of this group are characterized by a long pro-domain. This long amino terminal domain is a protein-protein interaction platform that allows for the recruitment of other pro-caspases. When two pro-caspases bind at their N-terminal pro-domains, they form an activating protein complex. Initiator caspases that contains the N-terminal caspase-activating recruitment domain, or CARD, are caspases-1, -2, -4, -5, -9, -11, and –12. In contrast, caspases-8, and –10 have short, non-enzymatic, N-terminal, death effector domain, DED. These executioner caspases are responsible for the majority of the cellular destruction associated with apoptosis.

When two pro-caspase-8 molecules are brought into close proximity, for example, when they are bound by FADDs, one molecule of pro-caspase-8 will proteolytically cleave the other, and vice versa (see Figure 3). The caspases' cleavage site is defined by specific aspartate residues in the protein structure that are dependent upon critical cysteines located at the active enzymatic site on each caspase[21]. Proteolytic activation of caspase-8 generates an amino terminal prodomain component that remains bound to FADD and two peptide fragments, p20 and p10, that are released into the cytoplasm. The p20 and p10 domains form a tetramer of two

p20-p10 heterodimers. Each tetramer contains two catalytic sties that contain critical cysteine residues that are necessary for the proteolytic cleavage of substrates [21]. This auto-proteolysis is important in releasing the active caspase-8 from the DISCs found on the cytoplasmic tail of the death receptors. The released caspase-8s are now free to proteolytically activate cellular substrates inside the cell that are important in promoting the apoptotic signaling pathway. As seen in Figure 3, some examples of caspase-8 substrates are; caspase-3, BID, actin, and the cytoskeleton of the cell. Caspase-3 and BID are less likely to be found near the DISC, however they are important components of apoptotic signaling downstream of caspase-8. An active caspase-8 that is still attached to FADD, however, can still cleave the substrates such as protein kinase RIP, actin, and components of the cytoskeleton. Moreover, when the cytoskeleton is cleaved near the death receptor, Fas, internalization is promoted [21].

Active caspase-8 promotes the cleavage of various downstream caspases, such as caspase-3, which in turn, proteolytically activates caspase-6 and caspase-7 as shown in Figure 3. Caspases-6 and -7 lack DD and DED, thus they cannot bind to FADD and activate the upstream apoptotic signaling pathway [21]. The activation of caspases-6 and -7 leads to the degradation of various cellular components, for example, caspase-6 cleavage of nuclear lamins, and caspase-3, cleavage of cytoskeletal proteins such as actin, gelsolin, and fodrin. Proteolytic degradation of these cellular elements leads to the characteristic cell shrinkage and membrane blebbing of apoptotic cells. Caspase-3 also activates caspase-7, which inhibits PARP, poly(ADP-ribose)polymerase, and thereby prevents PARP-dependent repair of damaged DNA (Figure 3) [21].

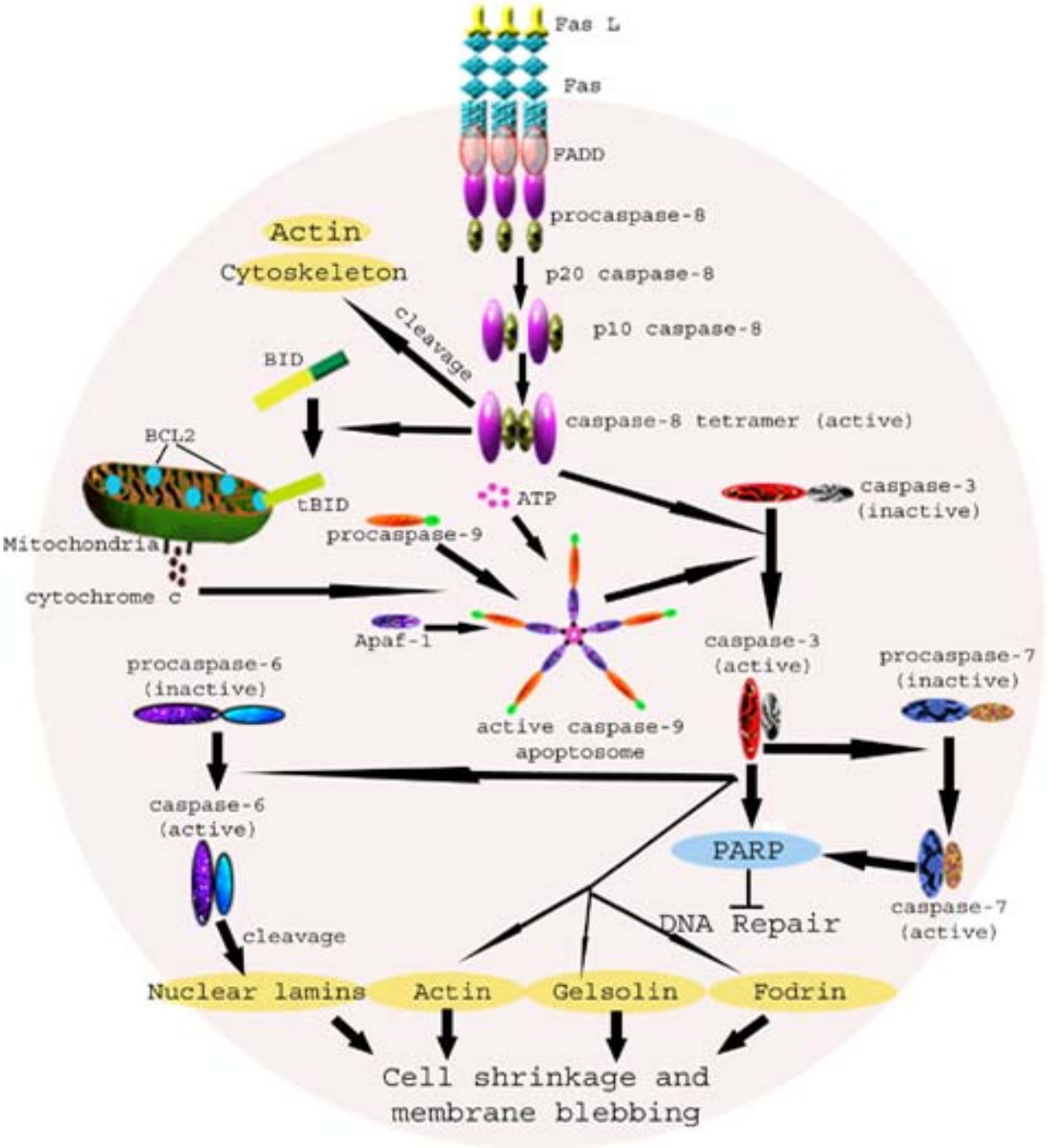

Figure 3: Apoptosis Caspase Cascade. When two or more initiator caspases are brought into close proximity via binding to the FADD/Fas complex they autoproteolyticaly cleave each other at specific aspartate residues. This releases their active catalytic subunits (p10 and p20). These subunits heterodimerize into the active caspase complex. This complex is now free to cleave downstream executioner caspases (caspase-3, and -7), proapoptotic agents, as well as cytoskeletal elements. In addition, the initiator caspases (caspases-8,-10) cleave proapoptotic agents such as BID and generates the active truncated form, tBID. In turn, tBID forms a complex with anti-apoptotic agents (BCL2) and disrupts the transmembrane potential of the mitochondria. Disruption of the mitochondrial membrane potential mediates the release of cytochrome c, a pro-apoptotic agent, into the cytoplasm. Cytochrome c forms a complex with an apoptosis protease activating factor (Apaf-1) that recruits and activates initiator caspase-9 to form the apoptosome. In turn, the apoptosome activates other executioner caspases (caspase-3,-7), as well as inhibits DNA repair by cleaving poly(ADP-ribose)polymerase (PARP) along with caspase-7. Degradation of cellular component (nuclear lamins) by executioner caspase-6 along with cleavage of cytoskeleton proteins (actin, gelsolin, fodrin) by executioner caspase-3 leads to the characteristic cell shrinkage and membrane blebbing of the apoptotic cell.

Methodology for Analyzing Apoptosis

Morphology

Observing the morphology of cells is an approach to analyzing and determining whether a cell is undergoing apoptosis. As mentioned previously, cells undergoing apoptotic cell death detach from the cellular substrate (if it is an adherent cell line), shrink in volume, demonstrate membrane blebbing, and form condensed chromatin masses due to DNA fragmentation [26].

DNA Degradation

The DNA fragmentation associated with apoptosis can be used as a biochemical marker of the apoptotic process. Agarose gel electrophoresis of the genomic DNA from apoptotic cells will appear as a ladder of DNA fragments on the gel that are integral multiples of ~180 base pairs due to the cleavage of DNA at internucleosomal sites by CAD. [27-29] These DNA strand breaks can also be detected by enzymatic labeling using the terminal deoxynucleotidyl transferase-mediated nick end labeling (TUNEL) method. The broken ends of DNA are sites of attachment for fluorescent-labeled dUTP in the presence of the terminal deoxynucleotidyl transferase enzyme. Once the nicked DNA ends are labeled, the emitted green fluorescence can be detected by flow cytometric analysis, fluorescent microscopy, or fluorometry [28, 30].

Caspase Activation

Specific caspases that are activated during the process of apoptosis can be measured using several methodologies. Caspase-3 can be quantitated by spectrophotometrically measuring the enzymatic cleavage of the chromophore pNA (pNitroanaline) from the caspase-3 substrate DEVD-pNA [31]. Caspase-8, caspases-9, and –6 can also be detected using fluorometric assays similar to the caspase-3 assay [31]. For example, caspase-9 and –6, when activated, will cleave

the substrate LEHD-AMC. The free AMC (amino-methyl-coumarin) can then be quantitated by fluorometric analysis [32, 33].

Phosphatidyl serine exposure

During apoptosis, the outer cell membrane undergoes numerous changes, including the exposure of phosphatidyl serine on the surface of the cell. It has been implicated that the presence of phosphatidyl serine on the cell surface acts as a signal for the removal of apoptotic cells by phagocytes [34]. Binding of phosphatidyl serine by a phosphatidyl serine receptor located on a phagocyte, triggers the phagocytic removal of the apoptotic cell. Thus, quantitation of phosphatidyl serine can be used to quantitate the apoptotic process. This can be accomplished using the phospoholipid binding protein, Annexin A5, that has been fluorescently labeled [35]. The advantages of detecting apoptosis by phosphatidyl serine exposure is that this technique can be performed *in vivo* since detection of the Annexin tag occurs on the outside of the cell [36].

PARP cleavage

The cleavage of known caspase substrates is an additional method of determining apoptosis in cells. One such substrate is Poly (ADP-ribose) Polymerase (PARP), a cellular enzyme involved in DNA repair. During apoptosis PARP, a 117 kDa protein, is cleaved by caspase-3 into 89kDa and 28kDa fragments. This proteolytic cleavage disrupts PARP-mediated DNA repair during apoptosis. The cleavage of this nuclear enzyme can be detected by Western Immunoblot analysis techniques using antibodies against PARP. [37, 38].

Cytochrome c release

Cytochrome c (an inner mitochondrial membrane protein) is released into the cytosol when the mitochondrial membrane potential is disrupted during apoptosis. The release of cytochrome c mediates the activation of downstream caspases that lead to apoptotic cell death. The translocation of cytochrome c from the mitochondria to the cytoplasm can be quantitated using a Western Immunoblot analysis. Differential centrifugation of cell lysates is performed to generate a mitochondrial and cytoplasmic fraction. These cell fractions are subsequently subjected to SDS-PAGE, transferred onto PVDF membranes and probed with anti-cytochrome c antibodies to quantitate the apoptotic release of cytochrome c into the cytoplasm [32]. It can also be detected by immunofluorescence; where cells are fixed, permeabalized, incubated with a cytochrome-c antibody, and then a conjugated fluorescent secondary antibody, before viewing under fluorescent microscopy [39].

Posttranscriptional Gene Silencing

Posttranscriptional gene silencing (PTGS), also known as Homology-Dependent Gene Silencing (HDGS), is a nucleotide sequence-specific mechanism that can target both cellular and viral mRNAs for degradation [40]. PTGS was first discovered in plants when R. Jorgensen introduced trans-genes coding for chalcone synthase, the gene responsible for purple pigmentation in petunia plants. He hypothesized that introduction of this trans-gene would increase the pigmentation of the plant's flowers, however he discovered that induction of the trans-genes had the opposite effect. In fact, many of the plants produced white or variegated petals. These results suggested that the trans-gene and its endogenous homologue, the plants natural chalcone synthase, were being silenced and thereby resulted in the observed white

phenotype of the flowers petals. The link between the silencing of the exogenous trans-genes and the endogenous genes was termed trans-gene co-suppression [41, 42].

Other work has shown that both RNA and DNA viruses induce gene silencing in plants at the posttranscriptional level. By investigating the cellular mechanisms responsible for PTGS, it was theorized that transgene suppression was the natural defense mechanism plants used to suppress viral gene expression [40, 41, 43]. This theory is best supported by the fact that two different plant viruses have independently developed a mechanism to neutralize the PTGS defense mechanism and thereby making them more virulent to the host plants [43].

PTGS and RNAi

RNA interference was initially investigated in the nematode, *C. elegans,* by Fire and Mello [44, 45]. They observed that either sense or antisense orientated RNAs could inhibit gene function in the nematode. However, when double stranded RNA was employed, the gene silencing effect was roughly tenfold that of either single-strand RNA molecules. Fire and Mello interpreted this dsRNA-induced effect as a new cellular process and named it RNA interference or RNAi. Like PTGS, RNAi caused rapid and prolonged degradation of mRNAs produced by the homologous gene. These studies demonstrated a strong correlation between RNAi and PTGS, suggesting similar cellular mechanisms mediate these processes. Subsequent investigations have observed RNAi in insects, protozoa, and vertebrates[46-48]. Thus, RNAi appears to be an evolutionarily conserved cellular mechanisms that protects organisms from infection with exogenous genetic material, such as from an invading virus [41, 43].

RNAi

RNAi methodology is a very useful tool that can be used to determine the function of a particular protein by silencing the expression of the gene at the messenger RNA (mRNA) level and then observing the resulting phenotype [49]. RNAi is one of the most effective ways to silence genes to explore gene function because of its high specificity in degrading only the target mRNA and because it requires only a few molecules of the dsRNA per cell to silence gene expression [23,44]. Furthermore, RNAi also cosuppresses genes that are homologous to the original gene of interest. These homologous genes could include endogenous genes in the cell as well as exogenous genes that are introduced into the cell [43].

RNAi has many potential medical applications. For example, in the field of hematology, many clinical disorders are due to the loss of gene function via the deletion of genes or gene mutations [49]. In oncology, RNAi has many potential applications for tumor regression therapy including a new mode of adjuvant chemotherapy [49]. This strategy employs RNAi that targets oncogenes and transcriptional factors that may be responsible for dysfunctional signaling pathways involved in oncologic disease [49]. RNAi techniques can also be used to analyze gene function in developmental animal models by using embryonic stem cells [50]. Furthermore, RNAi methods have been used to study infectious diseases. For example, RNAi has been employed to inhibit both cellular and viral factors that promote human immunodeficiency virus (HIV) [49].

Mechanism of Action of RNAi

The ATP-dependent RNAi reaction is a two-step process that begins with the introduction of dsRNA into the cell either by conversion of foreign RNA into dsRNA or by

transfection of dsRNA into the cell (Figure 4). Once inside the cell, the dsRNA is recognized by a Dicer enzyme, a member of the RNase III gene family. This enzyme cleaves the dsRNA into small fragments of interfering RNAs (siRNAs) that are about 21-23 nucleotides in length with two nucleotide overhangs on the 3'end [44, 49]. In plants the siRNA can be used as a template for an RNA-dependant RNA polymerase (RdRP) to synthesize *de novo* dsRNA. This new dsRNA can be processed to generate additional siRNA, thus greatly amplifying this process [51, 52].

The second step, the effector step, begins when the siRNA is incorporated into a non-active nuclease complex called the RNA-induced silencing complex (RISC). The 500 kDa, mulitiprotein RISC complex contains a helicase, an endonucleolytic nuclease, an exonucleolytic nuclease, and a homology-searching activity related to *E. coli* recA. Once the siRNA is incorporated into the RISC complex it becomes activated. The activated RISC molecule then searches the cytoplasmic compartment for homologous mRNA using the anti-sense strand of the siRNA to act as a guide to identify target mRNAs by base-pairing interactions [53]. When the complex finds a complementary match, it degrades the homologous mRNA into single stranded RNAs (ssRNA) that are about 21-23 nucleotides in length (see Figure 4). This degradation of only the homologous mRNA into segments that are exactly the same length as the siRNAs, supports the theory that the siRNAs act as guides for the RISC molecule, making the process highly specific for target genes as previously noted. [41, 43, 44, 49]

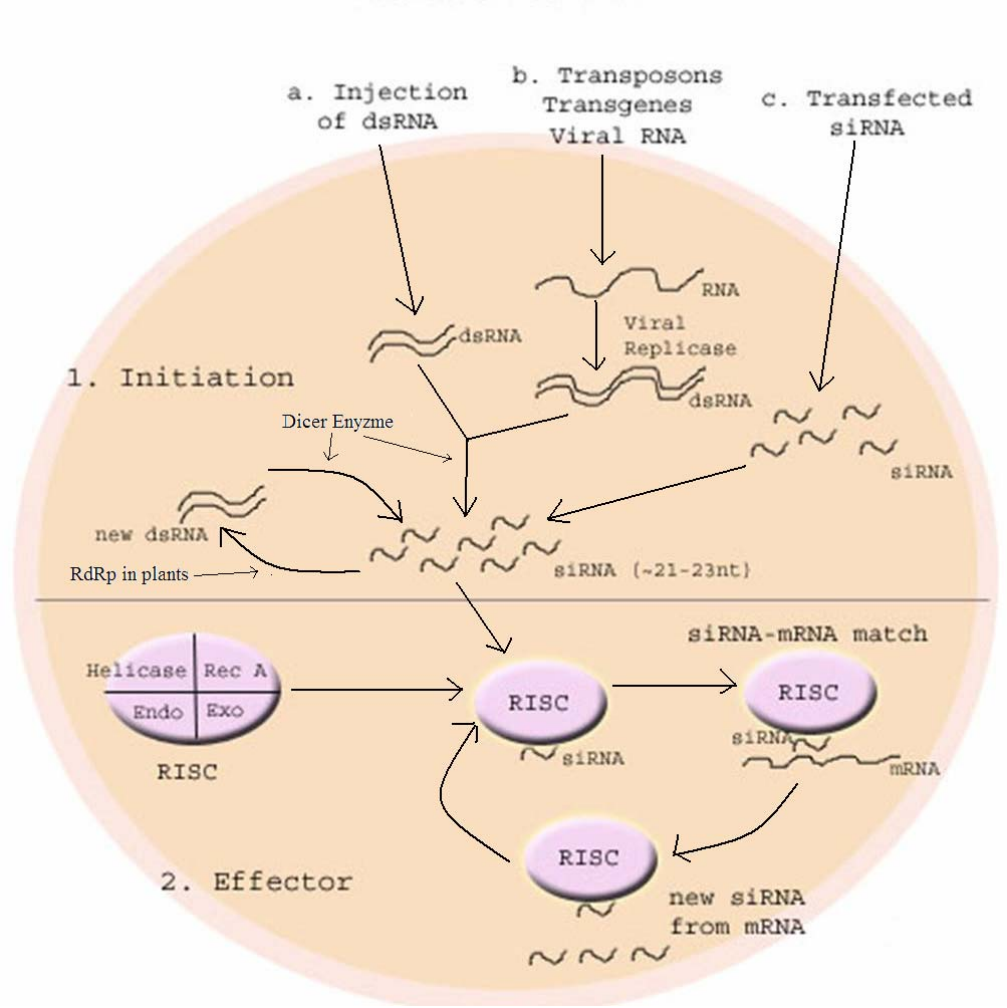

Figure 4: Cellular Mechanism of RNAi. The ATP-dependent generation of RNAi is a two-step process that begins with the introduction of dsRNA into the cell by transfection of dsRNA; induction of transposons, transgenes, or viral RNA or by transfecting siRNA directly into the cell. A secondary step to convert foreign single stranded RNA into dsRNA is performed by replicases such as a viral replicase as in the case of viral RNA induction. The dsRNA is then cleaved into small interfering dsRNA's (siRNAs) by Dicer enzymes. In plants the siRNA can be used as a template for an RNA-dependent RNA polymerase (RdRp) to synthesize additional dsRNA which is then cleaved by the Dicer Enzymes. The second step, called the effector step, begins with the incorporation of siRNA into a non-active nuclease complex called the RNA-induced silencing complex or RISC. The RISC molecule contains a helicase, an endonucleolytic nuclease (Endo), an exonucleolytic nuclease (Exo), and a homology-searching activity related to *E.coli's* Rec A (Rec A). When RISC becomes activated with incorporated siRNA, it searches the cytoplasmic compartment for homologous mRNA using the anti-sense strand of the siRNA to act as a guide for target mRNA via base-paring interactions. Once the RISC molecule finds a complementary match, it degrades the homologous mRNA into single stranded RNAs that are about 21-23 nucleotides in length. These new siRNAs can now be recycled into the RISC molecule and serves as templates to further increase mRNA degradation.

IFN Response and siRNAs

In mammalian cells, RNAi is not the only anti-viral response that can be activated with dsRNA. Another cellular response to the introduction of foreign RNA, called the interferon response (IFN), is mediated by a RNA-dependent protein kinase (PKR)/2'5'oligoadenylate synthetase (2'5'AS), that utilizes dsRNAs that are 30 nucleotides and longer, as opposed to the 21~23 nucleotides employed in RNAi. These long dsRNAs induce the IFN response which in turn, activates a non-specific inhibition of gene expression by silencing all mRNAs and frequently leads to apoptosis in mammalian cells [40]. Once PKR detects the presence of long dsRNA, it represses cellular translation by phosphorylating eukaryotic initiation factor 2α (EIF2α), while dsRNA induces 2'5'AS to produce a molecule that activates RNAseL, which non-specifically targets all mRNAs for degradation [49, 54]. The ultimate outcome of this process is the induction of cell death via apoptosis. siRNAs that are approximately 21 nucleotides in length are too small to engage the PKR/2'5'AS or activate the IFN response and thus are able to mediate gene-specific silencing.

To prevent the IFN response in mammalian cells when RNAi methodology is employed, scientists use synthetically produced double stranded siRNAs, dsRNA digested with *Escherichia coli* RNase III or, short hairpin RNA (shRNA) that are 21-23 nucleotides in length [54, 55]. The generation of suitable siRNA for gene silencing experiments poses a problem since numerous siRNAs must be screened to identify products that effectively silence specific mRNA expression.

The use of *E. coli* RNase III or recombinant human Dicer (re-hDicer) to cleave dsRNA is an effective means of generating sufficient amounts of heterogeneous siRNA's (hsiRNAs) for RNAi experiments using mammalian cell lines. Re-hDicer digests long dsRNA into 21-23 nucleotide siRNA with the appropriate 5'phosphate and two nucleotide (nt) overhangs at the 3'

ends that are required for RNAi activity. The processing of long dsRNA into a heterogeneous population of siRNA dramatically increases the effectiveness of gene silencing and reduces the need to screen individual siRNAs [55]. Recombinant human Dicer generates a more uniform population of 21-23 nt siRNAs as compared to *E.coli* RNase III. [56].

Short hairpin RNAs (shRNAs) have also been used to induce RNAi. These shRNAs allow for both strands of the siRNA to be expressed as a single RNA molecule. When introduced into the cell, the endogenous Dicer enzyme cuts the hairpin loop into siRNA, enabling it to associate with the RISC complex [54]. The use of shRNAs that are made endogenously in a siRNA expression vector facilitates cell transfections using a transgenic or viral delivery system. Since shRNA's can be endogenously expressed *in vivo*, they are being used to create continuous cell lines in which RNAi is used to stably suppress gene expression in mammalian cells [51].

Methodologies to Analyze RNAi

siRNA-mediated gene silencing is highly specific for gene targets since nucleotide mismatching of one to two nucleotides within the target gene sequence, results in a loss of gene silencing. To confirm that target genes have been silenced, DNA microarray analysis, western immunoblot analysis, northern analysis, and cellular fluorescence of expressed target genes (containing fluorescent tags) can be employed [49]. In DNA microarray analysis, DNA from experimental and control cells are arrayed on a glass slide. mRNA is isolated from treated cells and used to synthesize fluorescently labeled cDNA probes. The probes are then competitively hybridized to the DNA array and the fluorescent signal is analyzed as a ratio between control and experimental samples [57, 58].

Western blot analysis is used to detect the level of target gene expression by immunoblotting procedures. Cellular protein is extracted from the cells and resolved on SDS/PAGE gels and then transferred onto PVDF (polyvinylidene difluoride) membranes by electroblotting. Antibodies specific for the protein are used to reveal the level of target gene expression using fluorescent or chromogenic methods [56].

In Northern blot analysis the relative level of mRNA of a target gene is analyzed and quantified. The isolated mRNA is electrophoretically separated on an agarose/formaldehyde gel and then transferred onto nylon membranes. The membranes are then hybridized with radioactively labeled gene probes and autoradiography is performed to quantitate the level of gene expression. [40].

The effects of siRNA can also be detected *in vitro* by using an expression plasmid containing a fluorescent reporter gene. The expression plasmids contain a reporter gene, such as EGFP (enhanced green fluorescent protein) or luciferase that is fused to the gene of interest. Cells are co-transfected with the expression plasmid and siRNAs. The fluorescence of the reporter genes protein is analyzed by fluorometric methods and compared to controls. This comparison provides a quantitative analysis of gene silencing in the cells. The lower the fluorescence, the more RNAi activity present, and the greater the degree of gene silencing [54].

CHAPTER 2

THY28 GENE

Previously in our lab, a gene product was isolated during a screening procedure designed to identify cellular proteins that mediate avian lymphocyte apoptosis [28]. The isolated gene encodes a 242 amino acid protein referred to as cThy28 (GenBank accession number U34350), which shares greater than 90% amino acid similarity with several mammalian homologues [28]. cThy28 contains a nuclear-localization domain and is a phosphoprotein with potential glycosylation, myristolation, and kinase phophorylation sites, suggesting that it might have a functional role in the nucleus of lymphocyte cells [28, 59]. When the level of expression of cThy28 was screened in various tissues it appeared to be elevated in lymphoid tissue compared to levels in various other tissues including brain, liver, kidney, muscle, and small intestine [28]. Analysis of bursal lymphocytes undergoing apoptosis revealed that the cThy28 was proteolytically degraded as a function of time; however the role of this proteolysis in the apoptotic process remains unknown.

Recently, molecular cloning of mouse Thy28 (mThy28) was reported. In this study the genomic organization of mThy28 was analyzed [59]. In the 5' flanking region, a basal promoter activity and a negative regulator of promoter activity were found, along with a CCAAT box. The mThy28 cDNA encodes a protein that is 226 amino acids in length that is highly homologous (87%) to cThy28's 242 amino acids. The fact that mThy28 is a nuclear localized protein was confirmed by transfecting HEK 293T cells with a mThy28/EGFP construct and observing nuclear localized fluorescence [6, 60]. In the chicken, expression of cThy28 was highest in the immune organs including the bursa of Fabricius, thymus, and spleen; however, in the mouse

mThy28 is expressed in moderate amounts in the spleen, thymus, liver, kidney and the highest expression level was found in the testis [60]. Furthermore, it was shown that induction of apoptosis in Ramos B lymphomas resulted in a reduction of mThy28 expression at the mRNA and protein level [60].

hThy28

In the current study, the human homologue of cThy28, hThy28, was isolated to explore the correlation between Thy28 and apoptosis. The hThy28 cDNA, which included a 446 nucleotide 5'untranslated region (UTR), a 678 amino acid coding region, and a 198 nucleotide 3' UTR, was isolated from HeLa cells using RT-PCR (Figure 5). Primers used for the PCR reaction were based on the reported nucleotide sequence of HSPC144, a human homologue of cThy28 that was isolated from a CD34+ hematopoietic stem/progenitor cell (HSPC) stem cell library. hThy28 is a 225 amino acid protein that has an 80% amino acid identity to cThy28. A number of predicted structural motifs for the hThy28 protein were found by using ScanProsite (http://au.expasy.org/tools/scanprosite/). These predicted structural features include several casein kinase II phosphorylation sites, as well as a N-linked glycosylation site, three protein kinase C phosphorylation sites, a tyrosine kinase phosphorylation site, two N-myristoylation sites, and an amidation site as shown in Table 1 [61]. Two nuclear localization signals were predicted to be at amino acid position 3-7 and 21-24 as indicated in Figures 5 and 7 [62].

Table 1. Structural Motifs of hThy28

Feature	Characteristic	Nucleotide position
Length of cDNA	1323 bp	
5′ UTR	446 nucleotides	1-446
3′ UTR	198	1125-1323
Start codon	ATG	447-449
Stop codon	TAA	1122-1124
Poly adenylation signal	AATAA	1261-1265
	Amino acid motif	**Amino acid position**
Nuclear localization signals	RPRKR	3-7
	KRTK	21-24
N-linked glycosylation site	NLSS	52-55
Protein Kinase C	SdK	14-16
Phosphorylation sites	SgK	19-21
	SsK	150-152
Casein Kinase II	SgsD	12-15
phosphorylation sites	TktE	23-26
	SepE	61-64
	SrlE	65-68
	SieD	76-79
	TcwD	88-91
	TqfE	138-141
	SskE	150-153
	SkeD	151-154
	SmvD	159-162
	TqeE	209-212
	SleE	218-221
Tyrosine kinase phosphorylation site	KlgeEaffY	106-114
N-myristoylation sites	GTsgSD	10-15
	GSdkGL	13-18
Amidation site	sGKR	19-22
Sumo sites	AKVE	33-36
	MKSE	59-62
DUF589 site	---	54-221

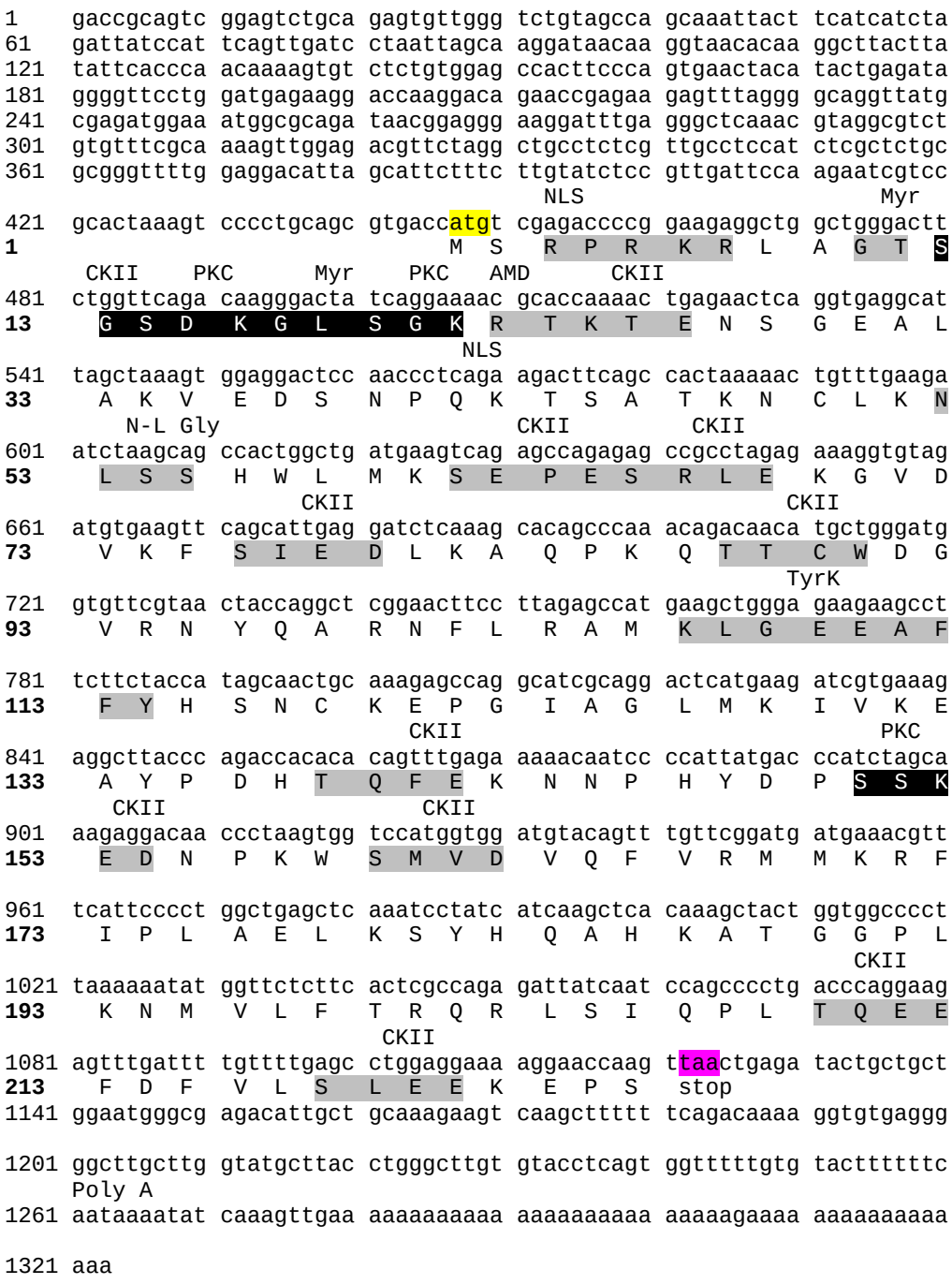

Figure 5. Nucleotide Sequence and Predicted Protein Translation of hThy28 (HSPC144) Demonstrating Structural Motifs. The nucleotide sequencing is numbered on the left margin with the amino acid sequence is numbered in bold below. Structural motifs are indicated by light shaded areas with the darker shaded areas representing overlapping motifs. Nuclear localization signal (NLS), protein kinase C phosphorylation site (PKC), casein kinase II phosphorylation site (CKII), tyrosine kinase (TyrK), myristoylation site (Myr), asparagine linked glycosylation site (N-L Gly), amidation site (Amd), and polyadenylation signal sequence (Poly A).

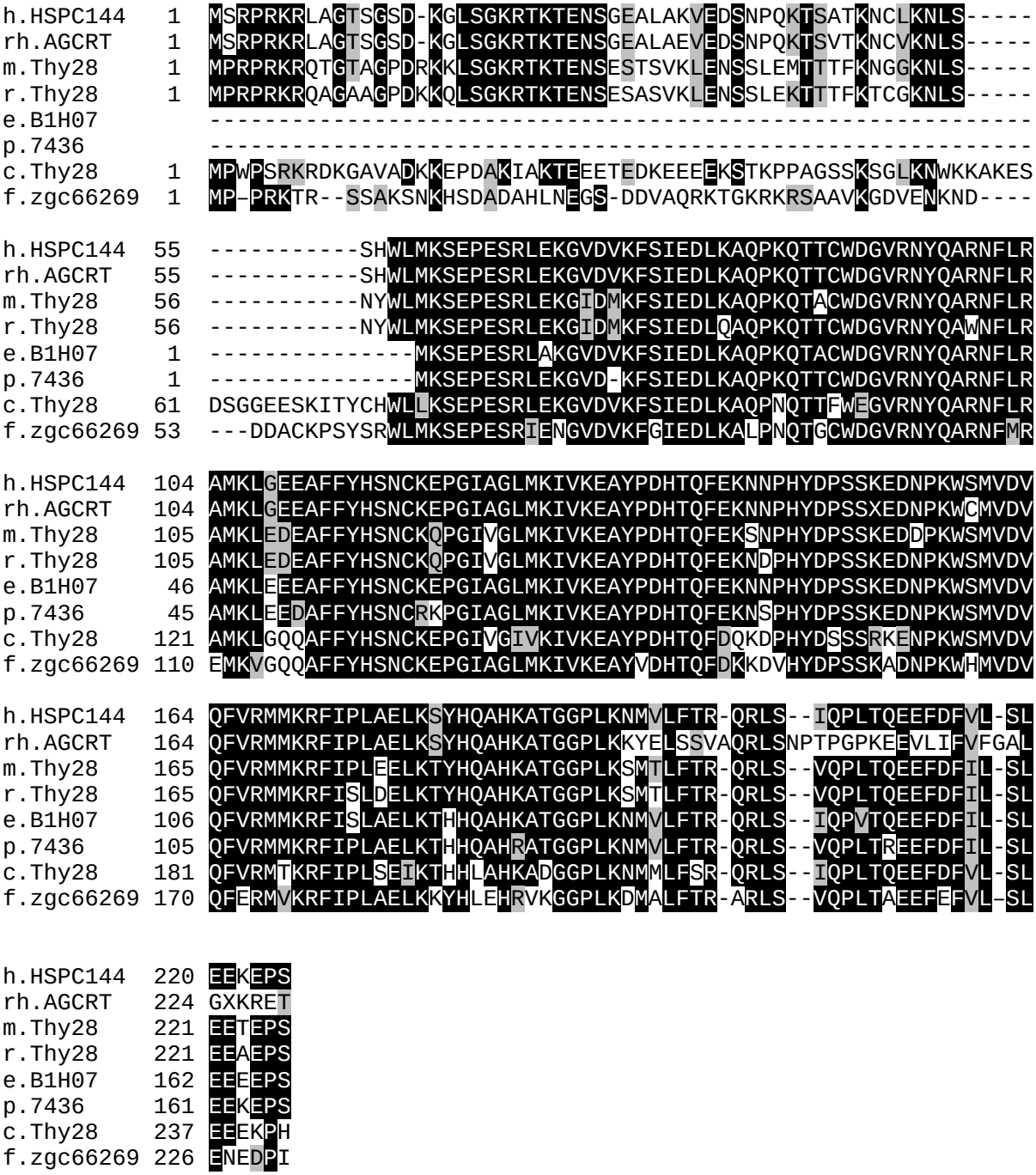

Figure 6: **Comparison of the Deduced Amino Acid Sequence for Homologues of hThy28**. Shown above is the amino acid sequence alignment for: human HSPC144 AF161493(h.HSPC144), Rhesus Monkey CB311693 (rh.AGCRT), Mouse Thy28 AB080370 (m.Thy28), Rat Thy28 BC064031 (r.Thy28), Horse HL0105B1H07 DN505600 (e.B1H07), Pig AW619394 (p.7436), Chicken Thy28 U34350 (c.Thy28), and Zebra Fish BC057500 (f.zgc66269). Areas of shared amino acid sequence identity are indicated by the dark shaded boxes and areas of shared amino acid similarity are indicated with light shaded boxes. Numbering of the amino acid sequences is located to the left of the amino acid sequence. Amino acid sequence alignment was performed using the multialignment program of the Clustalw series of programs[63]. Dashes represent areas for which there is no available sequence data.

```
Human HSPC144       1   MSRPRKRLAGTSGSDKGLSGKRTKTENSGEALAKVEDSNPQKTSATKNCL   50
Chicken cThy28      1   MPWPSRKRDKGAVADKKEPDAKIAKTEEETEDKEEEEKSTKPPAGSSKSG   50
Mouse mThy28        1   MPRPRKRQTGTAGPDRKKLSGKRTKTENSESTSVKLENSSLEMTTTFKNG   50
Rat rThy28          1   MPRPRKRQAGAAGPDKKQLSGKRTKTENSESASVKLENSSLEKTTTFKTC   50
Rhesus monkey       1   MSRPRKRLAGTSGSDKGLSGKRTKTENSGEALAEVEDSNPQKTSVTKNCV   50
Zebra fish 66269    1   MPPRKTRSSAKSNKHSDADAHLNEGSDDVAQRKTGKRKRSAAVKGDVENK   50
```

Figure 7: **Putative Nuclear Localization Signals in Thy28 Homologues.** Comparison of N-terminal amino acid sequences of h.HSPC144 (hThy28) with homologous proteins from chicken, mouse, rat, rhesus monkey, and zebra fish. Putative nuclear localization signals are underlined. Numbering of each amino acid sequence is located on the left and right margins.

Table 2: Homologues of HSPC144 (hThy28). Indicated below are the hThy28 homologues for various species (rhesus monkey, mouse, rat, horse, pig, chicken, and zebra fish). In addition, the GeneBank Accession Number, and Percent Amino Acid Identity are indicated.

Gene name	Species	Accession number	Percent amino acid Identity
HSPC144 (hThy28)	*Homo sapiens*	AF161493	1278/1278 (100%)
Agencourt_11834571	*Macaca mulatto*	CB311693	637/663 (96%)
mThy28	*Mus musculus*	AB080370	462/528 (87%)
rThy28	*Rattus norvegicus*	BC064031	456/521 (87%)
HL01015B1H07	*Equus caballus*	DN505600	647/728 (88%)
7436 Marc PBE	*Sus scrofa*	AW619394	495/545 (90%)
cThy28	*Gallus gallus*	U34350	149/185 (80%)
zgc:66269	*Danio rerio*	BC057500	166/203 (81%)

CHAPTER 3

MATERIAL AND METHODS

HeLa S3 Cell Culture

HeLa S3 cell cultures (ATCC #CCL-2.2) were plated at a concentration of 2.0 x 10^5 cells/ml in T-75 flasks containing 15ml Dulbecco's Modified Eagle's Medium (DMEM) supplemented, with 4.5mg/ml glucose,10% heat inactivated newborn calf serum, 50ug/ml streptomycin and 50 untis/ml penicillin. The cells were incubated in a humidified 5% CO_2 atmosphere at 37^{o}C.The cell concentration was determined using a Coulter Counter Model F (Beckman Coulter, Fullerton, CA). When plates were seeded at this concentration, they typically became confluent within three days.

Generation of hThy28 Constructs

The coding sequence of the hThy28 gene was isolated from HeLa cells using HeLa cell total RNA and RT-PCR methodology (PCR primers ATGhThy 28-5' and STPhThy28-3', Table 3). This PCR product was inserted into the pGEM-T Easy plasmid using a TA cloning strategy to generate the pGEM-T Easy/hThy28 construct. In turn, this construct was used for hThy28 nucleotide sequence analysis and the hThy28 insert was used as a template to generate ^{32}P-radiolabeled probes for Northern Analysis (see Figure 9).

An hThy28 construct was developed to use as a template for the generation of dsRNA using the pGEMTeasy vector (Promega, Madison, WI). The hThy28 insert was generated using PCR primers (T7-APNuc and T7-PNuc, Table 3) that incorporated the T7 nucleotide sequence (GCG TAA TAC GAC TCA CTA TAG GG) at the 5' and 3' ends of the hThy cDNA

(nucleotides 447 and 1124 respectively). This PCR product was ligated into the pGEMTeasy vector using a T/A cloning strategy (see Figure 10).

The hThy28/EGFP fusion protein, used to determine the subcellular localization of hThy28, was generated by ligating an hThy28 insert into the XhoI/BamHI site of the pEGFP-N3 plasmid (Clontech, Palo Alto, CA). The hThy28 insert was generated using a 5' PCR primer (XhoI/PvuII/Koz/ATG/hThy28-5', Table 3) that incorporated a Xho I restriction site and a Kozak recognition sequence at the 5' end of the gene (nucleotide 447). The 3' PCR primer (hThy28/dSTP/BamHI-3', Table 3) was designed to delete the stop codon and add a BamHI restriction site at the 3'end of the gene (nucleotide 1121) (Figure12).

Bacterial over expression of the hThy28 gene product was performed using the pET28b/hThy28 construct (Figure 11). The hThy28 insert was generated using PCR primers (BamATGhThy28-5' and STPBamhThy28-3', Table 3) that incorporate BamH1 restriction sites at both the 5' and 3' ends of the genes, respectively. This PCR product was ligated into the BamH1 sites of the pET28b expression vector (Novagen, Madison, WI). This construct was used to generate sufficient quantities of hThy28 for the generation of antibodies that were utilized in western immunoblot analysis.

Transcription of dsRNA

dsRNA hThy28 was synthesized from a PCR generated template (pGEM-T Easy hThy28-T7, Figure 10) that contained a T7 promoter at the 5'and 3' ends of the hThy28 using a Ribomax kit (Promega, Madison, WI.) Briefly, the reaction containing 1ug of PCR template, 5ul of T7 Enzyme Mix, 25mM rNTP's, and T7 Transcription Buffer in total reaction volume of 50ul. The reaction mix was incubated at 37^{o}C for 4 hours. Following the transcription reaction, the

single stranded RNA was annealed to generate dsRNA by heating the reaction mix at 70°C for 5 min and then cooling on ice for 5 min. The dsRNA was then treated with RQ1 DNase for 30 min at 37°C to remove the template DNA. The dsRNA was subsequently treated with Proteinase K, extracted with phenol/chloroform, ethanol precipitated, and quantitated spectrophotometrically. The integrity of dsRNA was evaluated by electrophoretic analysis on a 1.5% agarose gel.

Generation and Purification of siRNA

To generate hThy28 hsiRNA, Thy28 dsRNA was digested using the Recombinant Dicer Enzyme kit (Stratagene, La Jolla, CA) following the manufacturers protocol. In brief, 1ug of hThy28 dsRNA was digested with 0.5U of Dicer enzyme in a 10ul volume containing the Dicer reaction buffer. The reaction was incubated at 37°C for 18-20 hours. Undigested, high molecular weight dsRNA was removed from the reaction mix using a Micron YM-100 microcentrifugation column (Millipore Corporation).

hThy28 hsiRNA was evaluated by electrophoretic analysis using a 20% polyacrylamide gel and siRNA Markers (New England BioLabs, Washington, D.C.) as shown in Figure 8. The hThy28-hsi RNA generated using this procedure appeared as a single, 21bp band when analyzed by polyacrylamide gel electrophoresis.

Figure 8 Purification of siRNA of hThy28: From bottom to top: siRNA Markers (showing 25, 21,and 17 bp lengths from left to right) and hThy28 hsiRNA that was purified of dsRNA.

Transfection of Cells and Treatment with Cycloheximide

In this study, cycloheximide was selected as an apoptotic inducer among other pharmaceutical agents that were tested, including daunorubicin, camptothecin, and etoposide. The concentration employed in these studies was based on previous dose-response experiments that determined the minimum effective concentration needed in order to observe an increase in apopotosis while maintaining an optimal cell density for quantitative analysis. HeLa S3 cells were plated at a concentration of 2.5 x 10^5 cell per ml in a 12 well cell culture plate containing 1 ml of medium per well. The cells were incubated overnight, and on the following day the cell medium was removed and the cells were briefly washed with PBS. One ml of DMEM that was supplemented with 10% heat inactivated new born calf serum was added to each well. The cells were transfected by adding a 100ul volume of DMEM containing 2ul Lipofectamine 2000 (Invitrogen, Carlsbad, CA) plus 30ng of hsiRNA or the siRNA control Lit28i, and/or 1ug of hThy28/EGFP plasmid DNA. The cells were incubated for six hours and then the medium was removed and replaced with complete DMEM. To induce apoptosis, 10mM cycloheximide was added at this time and the cells were allowed to incubate for another 24 hours. After 48 hours of cell growth, the cultures were analyzed by crystal violet staining, immunoflourescent microscopy, Western blot analysis, or Northern blot analysis.

Crystal Violet Staining of Cells

Cell culture plates where stained with crystal violet to determine the relative cell density after the transfection procedures. The medium was removed and the cells were gently washed with PBS and then fixed with 90% ethanol for 5 minutes. The ethanol was removed and 0.1% crystal violet stain was added and incubated at room temperature for 5 minutes. The cells were

gently rinsed with water to remove excess stain. Quantitation of crystal violet staining was preformed using a Gel Doc Image Analysis System and Molecular Analyst software Version 2.1 (Bio-Rad Laboratories Hercules,CA).

Isolation of Cellular Protein from HeLa Cells

Following the treatment of HeLa cells in cell culture, cellular protein was isolated for Western Immunoblot analysis. The media was removed from the cells and they were washed 2 times with PBS. The cells were detached from the cell culture substrate by treatment with a solution of trypsin/EDTA (0.05% trypsin and 0.53mM EDTA in PBS) and harvested by centrifugation (1250 x g, 5 minutes, at 4^{o}C). The cells were lysed with 250µl of a detergent buffer containing proteinase inhibitors (5mM HEPES pH 7.5, 0.5 mM EDTA, 5 µg/ml pepstatin A, 10µg/ml leupeptin, 0.5 mM AEBSF, 5 µg/ml aprotinin, 0.5% Triton X-100, 0.1 mM sodium vanadate, 250 mM sodium fluoride, and 1.0 M NaCl) and subjected to brief sonication. The cell lysate was then centrifuged at 15,000 g for 15 minutes at 4^{o}C and the supernatant fraction was recovered. A Lowery protein assay was performed to determine the concentration of cellular proteins using bovine serum albumin as a protein standard. [64]

Generation of hThy28 Antibodies

To generate antibodies to the hThy28 protein, standard recombinant DNA techniques were employed to insert nucleotides 447-1124 of the hThy28 cDNA into the bacterial expression vector pET-28b (Novagen, Madison, WI) so sufficient amounts of the antigen could be generated for immunization protocols (pET28bhThy28, Figure 11). Antibodies directed against hThy28 were generated using a previously described protocol [28]. Briefly, PCR methodology was used

to incorporate Bam H1 restriction sites flanking the 5' ATG start codon and the 3' TAA stop codon of the hThy28s cDNA. This construct was ligated into the BamH1 site of the bacterial expression vector, pET-28b (Novagen, Madison, WI) (Figure 11) and transformed into *E.coli* BL21 (DE3) using standard recombinant DNA techniques. The hThy28 gene product was over-expressed in the bacterial cells by induction with 1mM IPTG (isopropyl-ß-D-thiogalactopyanoside) for four hours. 500ml of the bacterial cell culture were then harvested by centrifugation (8000 g, 10 minutes at 4^{o}C), lysed in 50 ml of lysis buffer (20 mM Tris pH 7.9, 500 mM NaCl, 5 mM imidazole, 0.1% Triton X-100, 100ug/ml lysozyme, 1 mM pepstatinA, and 10ug/ml aprotinin), and centrifuged at 39,000 g, 10 minutes at 4^{o}C. The supernatant fraction was briefly sonicated to shear bacterial DNA and stored at -80^{o}C [20]. The hThy28 protein was isolated from the bacterial lysate using metal chelation chromatography to affinity purify the expressed construct containing a 6-histidine tag at the amino terminus of the protein. The bacterial lysate was loaded onto a 2ml His-Bind column (Novagen, Madison, WI) and unbound bacterial proteins were removed from the column using a wash buffer (20 mM Tris pH 7.9, 500 mM NaCl, and 60 mM imidazole). The histidine-tagged hThy28 protein was eluted from the column (20MM Tris pH 7.9, 500mM NaCl and 1M imidazole) and dialyzed against a solution containing 50 mM Tris pH 7.4 and 500 mM NaCl. The protein was subsequently gel-purified via SDS-PAGE. Figure 13 demonstrates that hThy28 is purified to about 95 percent when isolated from the bacterial lysate using metal chelation chromatography. Figure 14 shows the time course of bacterial expression of hThy28 following IPTG induction and the purification of this protein using metal chelation affinity chromatography.

Antibodies to the recombinant hThy28 protein were generated in white Leghorn hens according to protocols approved by the University Animal Care and Use Committee. Eggs from

the hens were collected prior to the first injection, providing a pre-immune control. The hens where then injected three times intramuscularly (once every two weeks). The first injection contained 200ug of the gel-purified antigen solubalized in 500ul of PBS and 500ul of Freund's complete adjuvant. The second and third injections contained 200ug of the gel-purified antigen solubalized in 500ul of PBS and 500ul of Freund's incomplete adjuvant to boost the immune response. The immune eggs where collected one week after the last immunization.

IgY Antibodies to the recombinant hThy28 protein were isolated from the eggs using P.E.G. (polyethylene glycol) purification. In brief, the egg yolk was separated, washed with water, and diluted 4:1 with lysis buffer (10mM Tris-HCl, 100mM NaCl). 3.5% (wt./vol.) of P.E.G. 8000 (Fisher Scientific International, Hampton, NH) was added to the mixture and subjected to a brief centrifugation step (14000 x g, 10 minutes at 4^0C). The supernatant was filtered and 9% (wt./vol.) of P.E.G 8000 was added and another centrifugation was performed (10 minutes, 14000 x g at 4^0C). Both of the previous centrifugation steps were repeated once more before the supernatant was removed. The resulting pelleted fraction was resuspended in one half of the original yolk volume of lysis buffer and 0.2% NaN_3 was added. The antibody concentration was determined spectrophotometricaly and the relative purity of the antibodies was evaluated via analysis on a 12.5% SDS-PAG gel.

Western Immunoblot Analysis

For each sample, 50ug of protein from the cell lysate was electrophoretically separated using a 12.5% sodium dodecyl sulfate polyacrylamide gel (SDS-PAG, 8 x 10 x 0.15 cm gel) and electroblotted onto polyvinylidene difluoride (PVDF) membrane. The membranes were incubated over night at room temperature in a blocking solution (20mM Tris pH 8.0, 500 mM

NaCl, 1.5% Bovine Serum Albumin, BSA), washed with TTBS (20 mM Tris pH 8.0, 500 mM NaCl, 0.05% Tween 20) and incubated over night with 30ug/ml of primary antibody (chicken, anti-human hThy28, EE-1) in primary antibody buffer (TTBS containing 1% BSA and 1% goat serum). The membranes were subsequently washed in TTBS and incubated for 2 hours at room temperature with a 1:500 dilution of rabbit anti-chicken alkaline phosphatase conjugate (Sigma Chemical Company, St Louis MO) as the secondary antibody in secondary antibody buffer (TTBS containing 1% BSA and 1% goat serum). The membranes were washed in TTBS before adding the chromogenic substrate solution (100 mM Tris pH 9.5, 100 mM NaCl, 5 mM $MgCl_2$, 330 µg/ml nitro-blue tetrazolium chloride and 170 µg/ml 5-bromo-4-chloro-3'-indolyphosphate p-toluidine salt) to visualize the immunolocalized protein bands of interest on the membrane.

Northern Analysis

For Northern analysis of hThy28 expression, total RNA was isolated from HeLa cells using the TRIZOL Reagent (Life Technologies, Gaithersburg, MD) according to manufacturer's instructions. In brief, 1 ml of TRIZOL was added to $3.0x10^6$ cells/ml and mixed thoroughly prior to centrifugation at 12,000 g for 10 minutes at 4°C. The supernatant fraction was extracted with chloroform, and the RNA was precipitated using isopropyl alcohol and stored in 80% ethanol at -80°C. Prior to use, the RNA pellet was soluablized in 25 µl of nuclease-free water and treated with DNase using a DNA-*free* kit (Ambion, Austin, TX). The samples were incubated with the DNase Enzyme Mixture (Ambion, Austin, TX) at 37°C for one hour and 5µl of Inactivation Reagent (Ambion, Austin, TX) was added to remove the DNase enzyme. The samples were centrifuged at 10,000 g for 1 minute and the supernatant fraction containing the DNase-treated RNA was placed into a fresh tube and then quatitated spectrophotometerically.

Subsequently, 10ug of total RNA (DNase-treated) for each sample was electrophoresed on a 1.0% agarose/formaldehyde gel and then transferred to a nylon membrane using a PosiBlot pressure blotter (Stratagene, LaJolla, CA). Afterwards a UV Statalinker 2500 (Stratagene, LaJolla, CA) was used to cross link the transferred RNA onto the nylon membrane. To screen the blots for the presence of the hThy28 transcript, a ^{32}P-radiolabelled probe was generated as previously described [65]. The hThy28/pGEMT Easy plasmid (Figure 9) was digested with EcoR1 and the hThy28 insert was recovered by gel purification and used as a DNA template for ^{32}P-radiolabelling using a Prime-It kit (Stratagene, La Jolla Ca) according to the manufacturer's recommendation. The ^{32}P-GAPDH (glyceraldehyde phosphate dehydrogenase) probe was generated in a similar fashion using a highly conserved region of the chicken GAPDH gene (nucleotides 27–652) as a DNA template [65]. This radiolabeling procedure typically yielded a product with a specific activity of ~5x10^9 cpm/ug DNA.

The Northern blots were hybridized with the radiolabeled probe (1-5x10^6 cpm/ml) in a mixture containing 50% formamide, 5xSSPE, 5xDenhardts, 0.1% SDS and 50ug/ml denatured herring sperm DNA at 42^{o}C for 16 hours. Afterwards the blots were washed in a solution containing 2xSSC and 1.0% SDS and processed for autoradiography [65]. The autoradiographs where then scanned with a COHU High Performance CCD camera connected to an IS-1000 digital imaging system (Alpha Innotech Corporation, San Leandro, CA) and the intensity of the signals was calculated using Image-Quant (Version 3.3; Molecular Dynamics, Sunnyvale, CA) densitometry software.

RT-PCR (Reverse Transcription-Polymerase Chain Reaction)

The first step in the RT-PCR protocol was the reverse transcription reaction used to produce cDNA. 2.5 µg of total RNA was combined with 0.25 µg oligo (dT)12-18, 0.5 mM dNTP, and 1µg of random hexanucleotides, in a total reaction volume of 12 µl. The samples were then incubated at room temperature for 10 minutes, followed by 65^{o}C for 5 minutes and a quick chill on ice for 3 minutes, and then 45^{o}C for 2 minutes. Then the following reagents were added to each sample: RT synthesis buffer (50 mM Tris-HCl pH 8.3, 75 mM KCl, 3 mM MgCl2, and 10 mM DTT), 20 units of RNasin (Promega, Madison, WI), and 100 units of MMLV Reverse Transcriptase (Invitrogen, Carlsbad, CA). This reaction mixture was then incubated at 42^{o}C for 30 minutes, 50^{o}C for 20 minutes and 70^{o}C for 5 minutes.

The second step in the RT-PCR protocol was the amplification of the cDNA using polymerase chain reaction. 5µl of cDNA template was added to a PCR reaction containing: 20 mM Tris-HCl (pH 8.4), 50 mM KCl, 15 mM MgCl2, 0.2 mM dNTP, 1ul Hot Start Taq Polymerase, 0.2 µM upstream primer, and 0.2 µM downstream (shown in Table 3) in a reaction volume of 50µl. The PCR reaction was then incubated for 15 minutes at 94^{o}C to activate the Hot Start Taq Polymerase, followed by 30 cycles at 94^{o}C for 30 seconds, 58^{o}C for 30 seconds, 68^{o}C for 2 minutes, followed by an additional cycle of 68^{o}C for 5 minutes.

Caspase-3 Assay

A capase-3 assay was performed to detect apoptosis in HeLa cells. Approximately 3.0x10^{6} cells/ml were lysed in a buffer containing 10 mM HEPES (pH 7.5), 5 mM $MgCl_2$, 1 mM EDTA, 0.1% CHAPS, 20 µg/ml leupeptin, 10 µg/ml pepstatin, 1 mM AEBSF, and 10 µg/ml aprotinin. The samples were centrifuged at 15,000 g for 15 minutes at 4^{o}C and the supernatant

fraction was recovered and stored at -20^{o}C. A Lowery protein assay was used to determine the protein concentration in the cell lysates using bovine serum albumin as the protein standard. Triplicate 20µg aliquots of the protein lysate were incubated for 2 hours at 37^{o}C in an assay buffer containing the following: 100 mM HEPES (pH 7.5), 5 mM DTT, 10% sucrose, 0.1% CHAPS, and 500 µM fluorogenic caspase-3 substrate IX [(Z-Asp-Glu-Val-Asp)$_2$-Rhodamine 110 CalBioChem, Darmstadt, Germany]. The relative amount of fluorescence released from the substrate, as a result of caspase activity was measured using aVictor$^{3\ TM}$ multilabel counter (model #1420, PerkinElmer LAS Inc. Shelton, CT).

Densitometric Analysis of Data

Densitometric quantitation of protein bands on Western immunoblots, crystal violet staining of cultured HeLa cells, and PCR products in acylamide and agarose gels was performed using a Gel Doc Image Analysis System and Molecular Analysis Software (Bio-Rad Laboratories, Hercules, CA). Bands on autoradiographs or immunoblots were quantitated by measuring the relative optical density within a defined region (O.D. x mm^2), subtracting background values and expressing these data as a percentage of the maximum densitometric value. [28]

Preparation of Cells for Fluorescent Microscopy

HeLa cells were plated at a concentration of 2.5 x 10^5 cells/ml in 12-well cell culture plates containing 1ml DMEM complete media. Glass cover slips were placed on the bottom of the cell culture wells to allow for cell attachment. The cells where then transfected as described previously. Prior to fixation, the media was removed and cells were washed 3 times with PBS.

Cells were fixed in 2% formaldehyde in PBS for 5 minutes at room temperature and then washed 3 times with PBS. To permeabilize the cells, 0.5% Triton x-100 in PBS was added and incubated for 30 seconds at room temperature. The cells were washed 3 times with PBS and briefly dehydrated with acetone at 30^{o}C. 1ml of PBS containing Hoescht dye 33258 was added to the cells and allowed to incubate for 5 minutes at room temperature. The cover slips, with attached cells, were again washed with PBS 3 times. 1ml of PBS containing 100uM rhodamine labeled phallodin (Sigma, St. Louis MO) was added to cells and incubated for 40 minutes at room temperature. The cells were subsequently washed in PBS to remove excess stain and mounted on to slides with the anti-fade, p-Phenylenediamine (0.01%) (Sigma, St. Louis MO).

Statistical Analysis

The data presented, represents the mean of each treatment $\pm$ the standard deviation (SD) for each group. Data were analyzed using an analysis of variance (ANOVA) and a difference of $p < 0.05$ was considered to be statistically significant. Statistical difference among treatments was determined using Tukey Simultaneous Tests.

Table 3: PCR Primers Used to Generate Constructs

Construct	Primer Identification	Nucleotide Sequence of Primer
pGEM-T Easy/hThy28	ATGhThy28-5’	5’-ATG TCG AGA CCC CGG AAG AGC-3’
	STPhThy28-3’	5’-TTA ACT TGG TTC CTT TTC CTC C-3’
pGEM-TEasy/hThy28-T7	T7-APNUC	5’-GCG TAA TAC GAC TCA CTA TAG GGA TGC CCT GGC CGA GCA GAA AG-3’
	T7-PNUC	5’-GCG TAA TAC GAC TCA CTA TAG GGA GAT TAA TGT GGC TTT TCC TCT TCC-3’
pET28b/hThy28	BamATGhThy28-5’	5’-TTG GAT CCG ATG TCG AGA CCC CGG AAG AGG-3’
	STPBamhThy28-3’	5’-AGG ATC CTT AAC TTG GTT CCT TTT CCT CC-3’
pEGFP-N3/hThy28	hThy28/dSTP/BamHI-3’	5’-GGC GGA TCC ACT TGG TTC CTT TTC CTC CAG-3’
	XhoI/PvuII/Koz/ATG/hThy28-5’	5’-TCT CGA GCT CAG CTG GCC GCC ATG TCG AGA CCC CGG AAG AGG CTG-3’

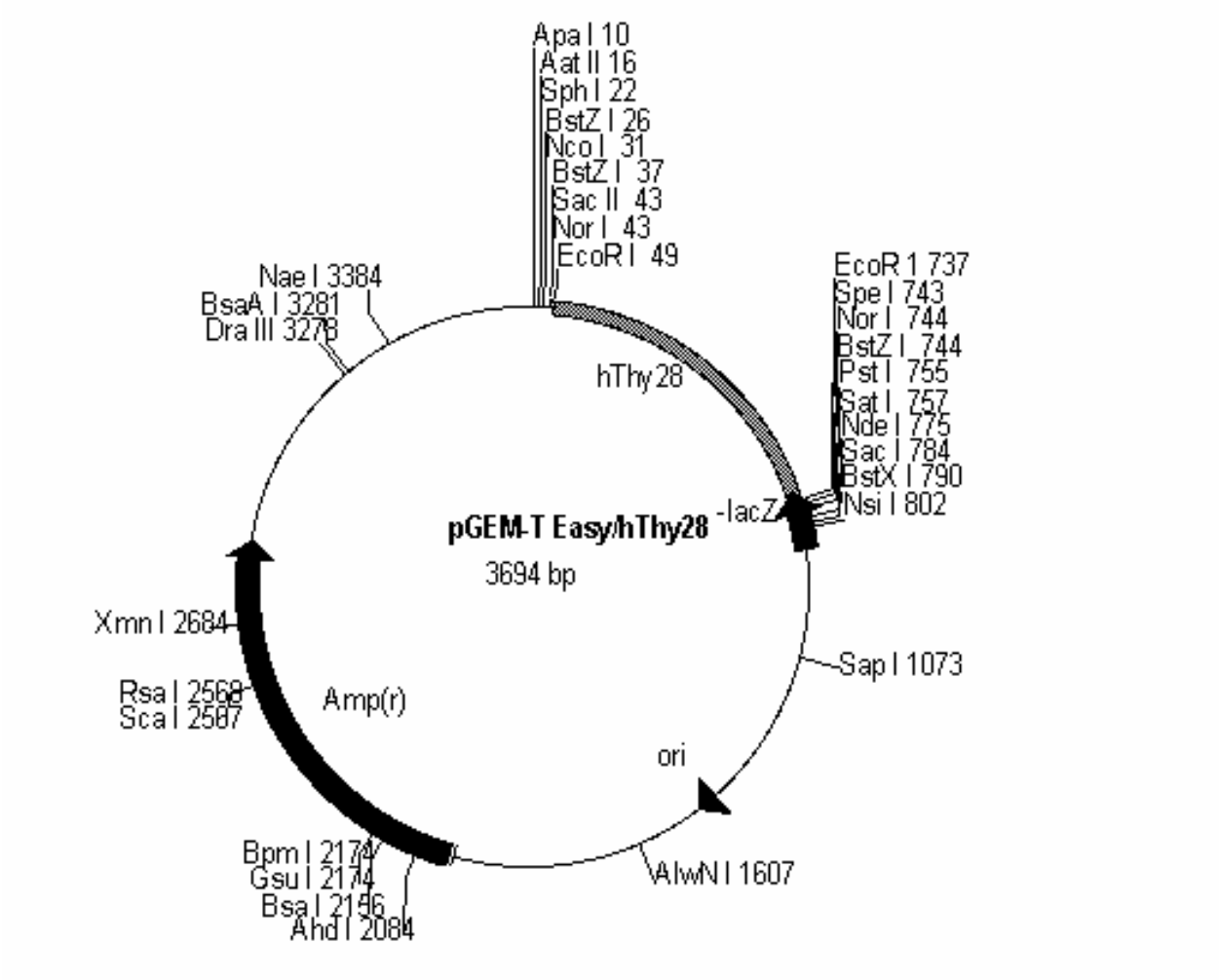

Figure 9: Generation of pGEM-T Easy/hThy28 Construct. The coding portion of hThy28 insert was generated using PCR primers (ATG hThy28-5' and STP hThy28-3', Table 3). This PCR product was ligated into the pGEMTeasy vector using a T/A cloning strategy.

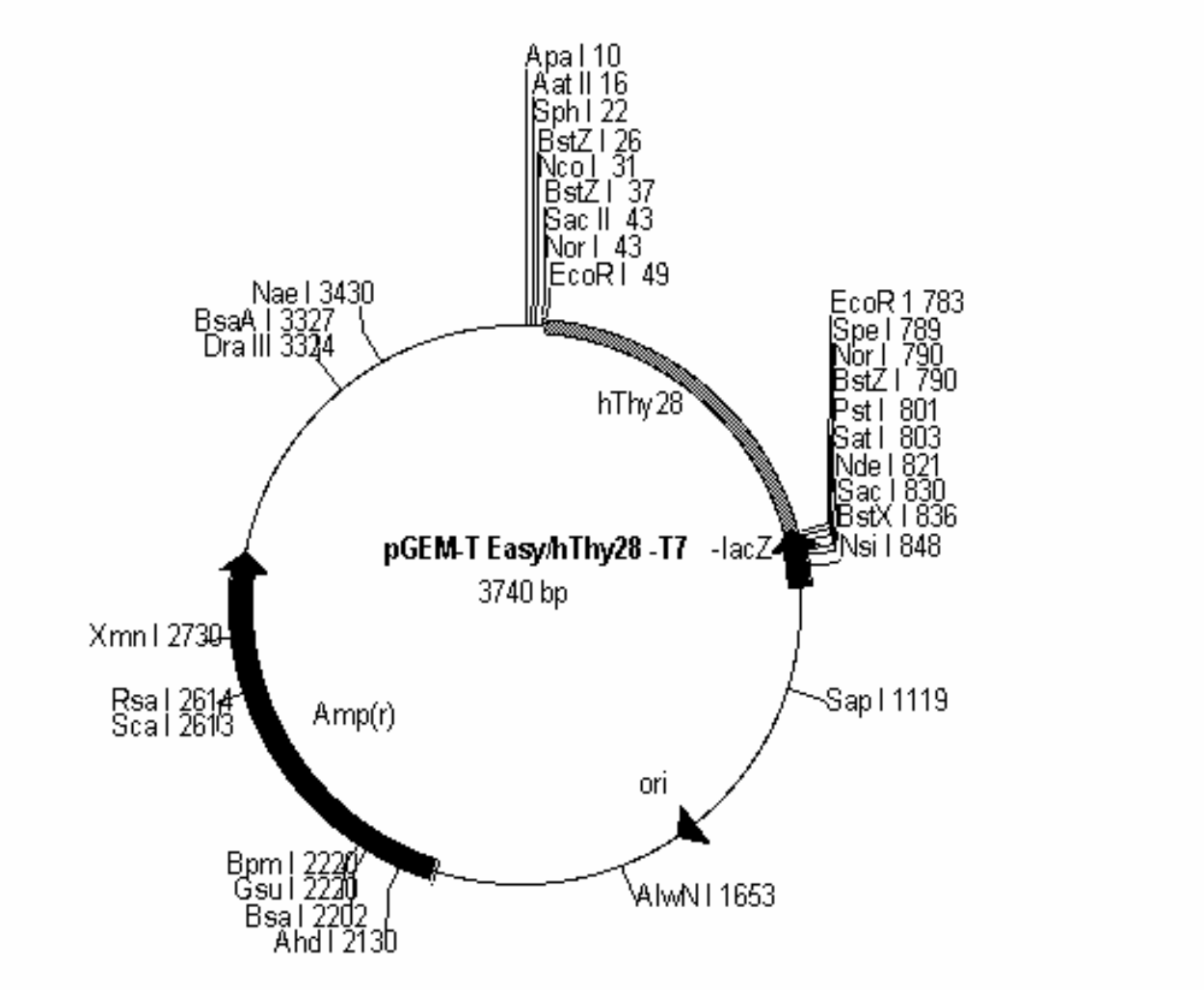

Figure 10: Generation of pGEM-T Easy/hThy28-T7 construct. The hThy28 insert was generated using the PCR primers (T7-APNUC-5' and T7-PNUC-3', Table 3) that incorporated the T7 nucleotide sequence at the 5' and 3' ends of the hThy28 cDNA (nucleotides 447 and 1124). This PCR product was ligated into the pGEMT-Easy Vector using a T/A cloning strategy.

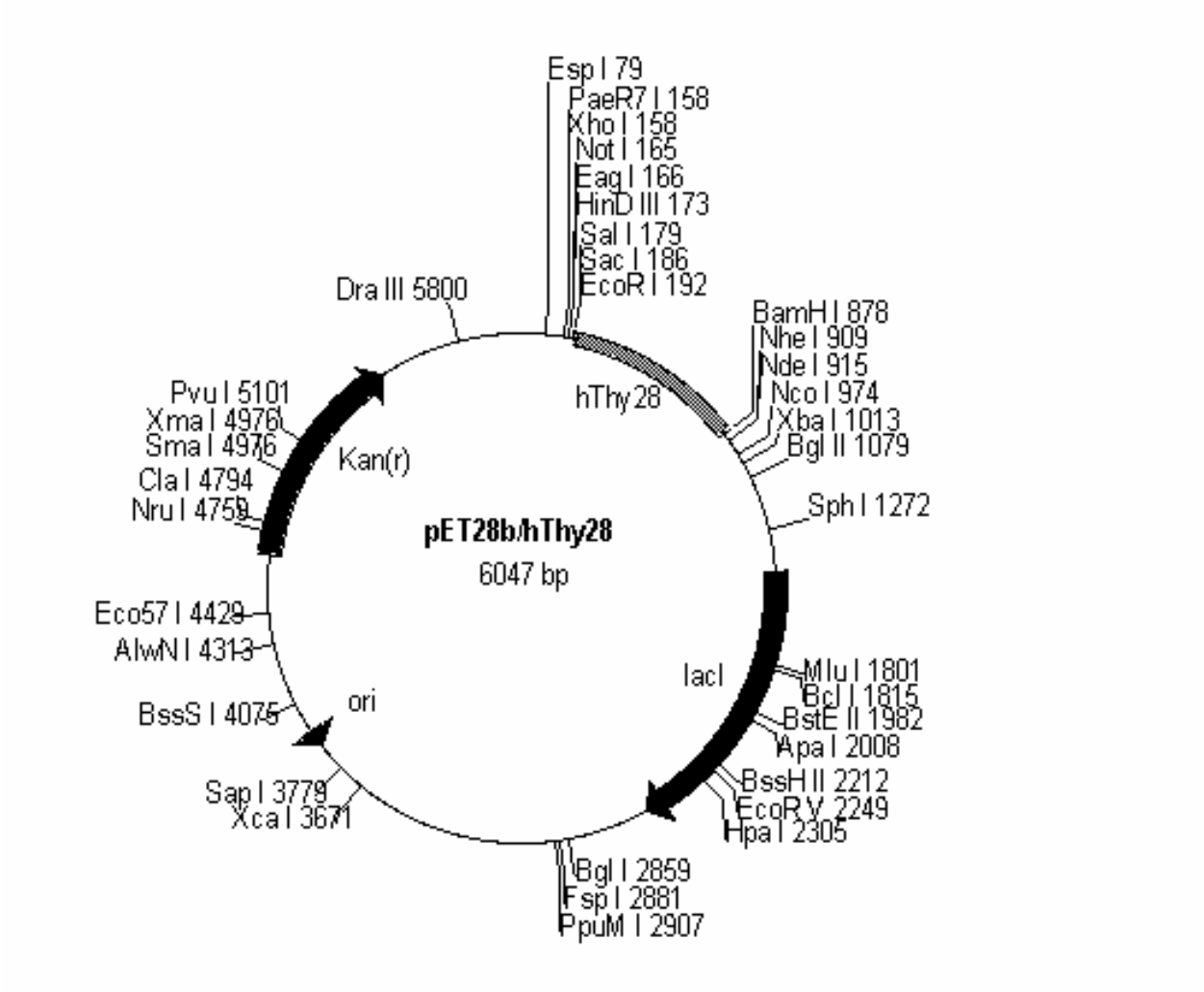

Figure 11: Generation of pET28b/hThy28 Construct. The hThy28 insert containing the coding region was generated using PCR primers (BamATGhThy28-5' and STPBamhThy28-3', Table 3) that incorporated BamH1 restriction sites at both the 5' and 3' ends of the genes. This PCR product was ligated into the BamH1 sites of the pET28b expression vector. This construct was designed for bacterial over expression of the hThy28 gene product.

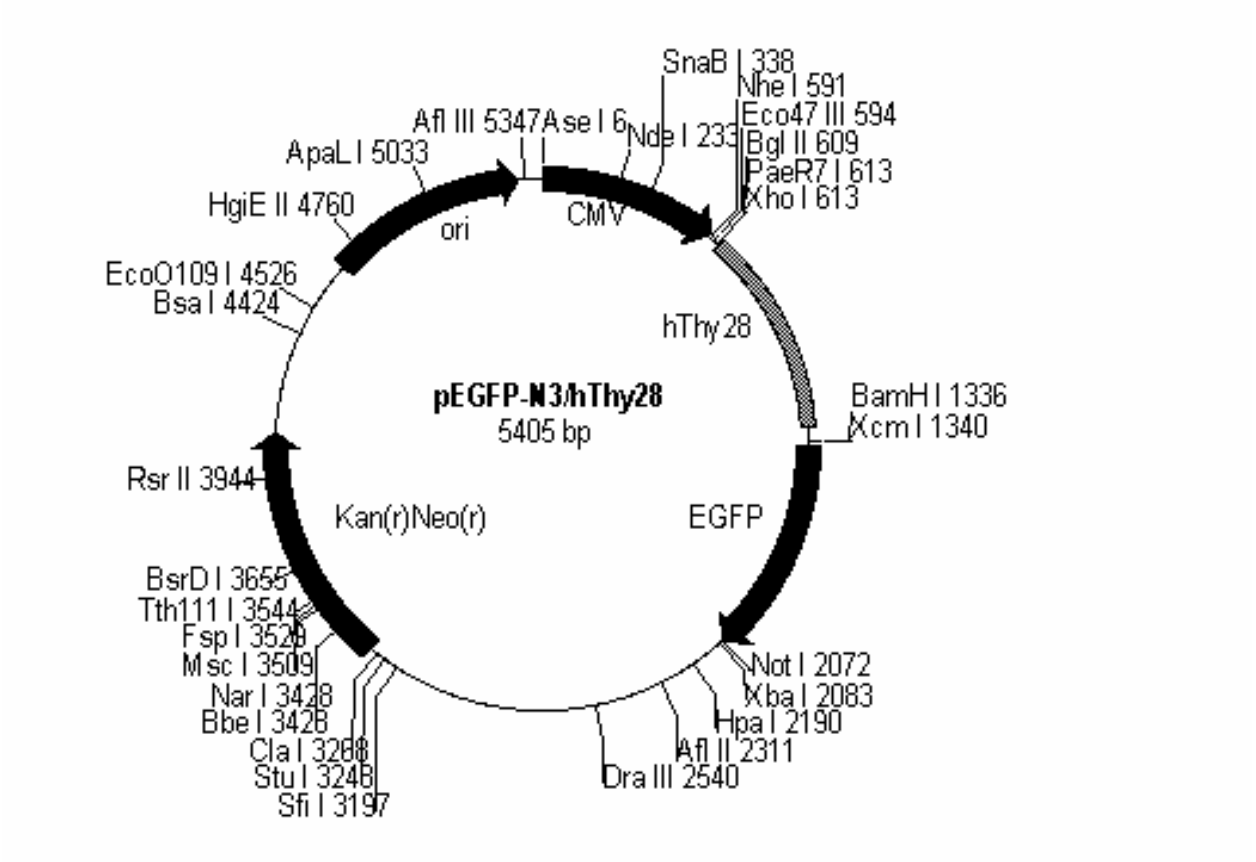

Figure 12: Generation of pEGFP-N3/ hThy28 construct. The hThy28 insert containing the coding region was generated using a 5' PCR primer (XhoI/PvuII/Koz/ATG/hThy28-5', Table 3) that incorporated a Xho I restriction site and a Kozak recognition sequence at the 5' end of the gene and the 3' PCR primer (hThy28/dSTP/BamHI-3', Table 3) was designed to delete the stop codon and add a BamHI restriction site at the 3'end of the gene (nucleotide 1121). This PCR product was ligated into the XhoI/BamHI site of the pEGFP-N3 plasmid to generate a hThy28/EGFP fusion protein.

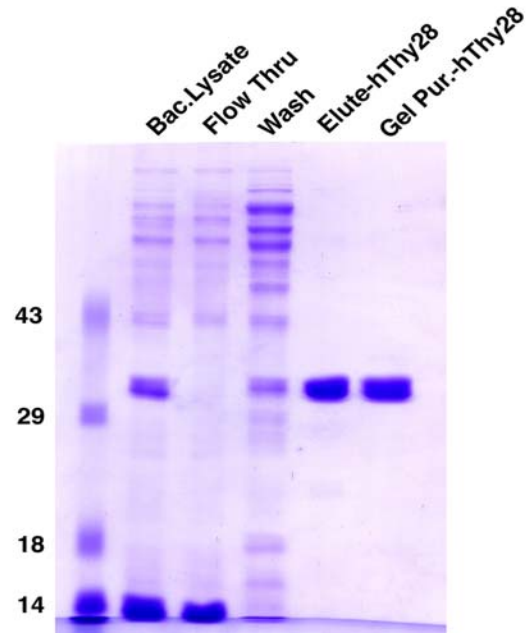

Figure 13: Purification of hThy28 Protein Using Metal Chelation Affinity Chromatography. Aliquots of the bacterial cell culture (Bac.Lysate) and chromatographic fractions including the material that failed to bind to the column during the loading of the bacterial lysate (Flow Thru), the column wash fraction (Wash), the fraction containing the eluted hThy28 (Elute-hThy28) and the eluted protein that was further enriched by gel purification using SDS-PAGE (GelPur-hThy28) were analyzed by SDS-PAGE and Coomassie Blue staining. Molecular weight markers expressed in kilodaltons are indicated on the left.

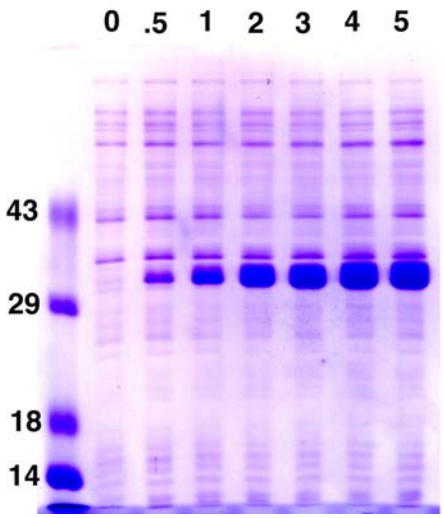

Figure 14: Time Course of Bacterial Induction of hThy28 Protein and Purification Using Metal Chelation Affinity Chromatography. Aliquots of the bacterial lysates were collected at 0, 0.5, 1, 2, 3, 4, and 5 hours after induction with 1 mM IPTG and analyzed by SDS-PAG and Coomassie Blue staining. Molecular weight markers expressed in kilodaltons are indicated on the left.

CHAPTER 4

RESULTS

Analysis of the Effects of hThy28-hsiRNA on HeLa Cells Undergoing Apoptosis

To analyze the effects of hThy28-hsiRNA on HeLa cells undergoing apoptosis, cells were grown in 12-well cluster plates and stained with crystal violet following treatment with cycloheximide (CHX), an inhibitor of protein translation that induces apoptosis in HeLa cells [66]. In Figure 15, Panel A demonstrates the crystal violet staining of cells in cell culture plates and Panel B graphically demonstrates the densitometric quantitation of cell staining.

Analysis of cell staining in Row I indicated that CHX and hThy28-hsiRNA (hsi) treatment had no significant effect on cell viability, while a combination of hsi and CHX resulted in a significant (45% decrease) loss of cells from the cell culture substrate. Cells in Row II were transfected with an hThy28/EGFP construct and subsequently treated with cycloheximide and hThy28-hsiRNA. This analysis demonstrated that CHX alone did not alter cell viability compared to control transfectants, although, hThy28-hsiRNA treatments resulted in a significant (19 % decrease) in cell viability. However, treatment of hThy28/EGFP transfected cells with hThy28-hsiRNA plus CHX resulted in a dramatic decline in cell viability (49% decrease). Cells in Row III were transfected with lit28i, a control siRNA, to demonstrate the specificity of the hThy28-hsiRNA treatment effect. These data show that CHX, hThy28/EGFP, and hThy28/EGFP plus CHX had no significant effect on cell viability compared to cells transfected with lit28i alone. Furthermore, lit28i treatment alone (Row III) had no significant effect on cell viability compared to control cells (Row I).

Nuclear Localization of hThy28 Gene Expression

HeLa cells were cultured on glass cover slips, transfected with the hThy28/EGFP construct or the EGFP control construct and viewed under fluorescent microscopy to observe the subcellular localization of the hThy28 gene product (Figure 16). Panel A of Figure 16 shows that green fluorescence was detected throughout the cell when HeLa cells were transfected with the EGFP expression vector that lacked the hThy28 insert. However, when cells were transfected with the hThy28/EGFP fusion gene construct, virtually all of the green fluorescence was restricted to the cell nucleus (Figure 16, Panel B). Moreover, intense green fluorescence was localized to the nucleolar region of the nucleus.

These observations were corroborated when HeLa cells were transfected with the hThy28/EGFP construct and stained with rhodamine-labeled phallodin, an actin binding reagent and Hoeschest dye # 33258, a nuclear staining fluorochrome (Figure 17). Panel A of Figure 17 demonstrates the nuclear/nucleolar localized green fluorescent staining of the expressed hThy28/EGFP, Panel B shows the red fluorescent staining of cytoskeletal elements, Panel C demonstrates the blue fluorescent staining of DNA in the nucleus, and Panel D is a composite image of Panels A-C. Panels E-H corresponds to the fluorescent images in Panels A-D, however, these cells were transfected with the hThy28/EGFP construct plus 30ng/ml hThy28-hsiRNA. Panel E clearly demonstrates a diminution in the green fluorescent staining of the nucleus and a dramatic loss in nucleolar fluorescent staining. The red fluorescent staining of the cytoskeleton and the blue fluorescent staining of the nucleus in Panels F and G, respectively are virtually identical to corresponding panels B and C.

Northern Analysis of hThy28/EGFP Gene Expression in Treated HeLa Cells

To confirm that the hThy28-hsiRNA treatment effectively inhibited the accumulation of hThy28 transcripts in HeLa cells, a Northern blot analysis was performed on cells that had been transfected with the hThy28/EGFP construct and treated with 30ng/ml hThy28-hsiRNA or 10mM cycloheximide (Figure 18). Panel A of Figure 18 is a Nothern blot autoradiograph of treated cells that shows the relative level of hThy28/EGFP expression compared to GAPDH. Panel B graphically demonstrates the densitometric quantitation of hThy28/EGFP expression relative to GAPDH for each treatment. These data clearly demonstrate that, compared to control transfectants (Con), hThy28-hsiRNA (hsi) treatment dramatically reduces hThy28/EGFP gene expression (a 23-fold reduction) while the lit28i control dsRNA fails to reduce hThy28 expression. Likewise, cycloheximide(CHX) treatment alone or in combination with lit28i fails to effectively inhibit hThy28/EGFP gene expression. When cells were treated with a combination of CHX and hThy28-hsiRNA, inhibition of hThy28/EGFP was comparable to that of hThy28-hsiRNA alone.

Analysis of Caspase-3 Activity in Treated HeLa Cells

A fluorescent caspase-3 assay was employed to analyze the effects of 10mM cycloheximide (CHX), 30ng/ml hThy28-hsiRNA (hsi), and 30ng/ml control RNAi (lit28i) on HeLa cell apoptosis (Figure 19). As shown in Figure 19, CHX, hsi, lit28i, or lit28i plus CHX treatment has no significant effect, compared to control cells, on activating caspase-3 activity. However, treatment of cells with hsi plus CHX elevated caspase-3 levels by approximately 50% and was statistically different from control cells. Treatment of cells with hsi alone was not significantly different from hsi plus CHX treatments or contol cells, although hsi treatment

tended to increase caspase-3 activity (34%, statistically nonsignificant) compared to control cells.

Western Immunoblot Analysis of Treated HeLa Cells

Western Immunoblot analysis was employed to confirm that the hThy28-hsiRNA treatment effectively reduced the amount of hThy28 protein in cells that had been transfected with the hThy28/EGFP construct and treated with hThy28-hsiRNA. As shown in Figure 20, the bacterial over-expression of hThy28/EGFP (the positive control, recomb hThy28) shows where the endogenous levels of hThy28 resolve on an SDS-PAG gel. As seen in the control (Con), endogenous levels of hThy28 are too low to be detected. However, cells transfected with the hThy28/EGFP construct (hThy28/EGFP) can be detected using Western Immunoblot analysis and the reduction of signal presented is dramatic when compared to cells that were transfected with hThy28/EGFP combined with hThy28-hsiRNA (hThy28/EGFP+hsi), while the hsi control, lit28i (hThy28/EGFP+lit28i), fails to reduce hThy28/EGFP expression. Also, cells that were treated with hThy28/EGFP plus EGFP-hsiRNA (hThy28/EGFP+hsiEGFP) showed a dramatic reduction in the expression of the hThy28/EGFP construct.

Crystal Violet Cell Staining

A

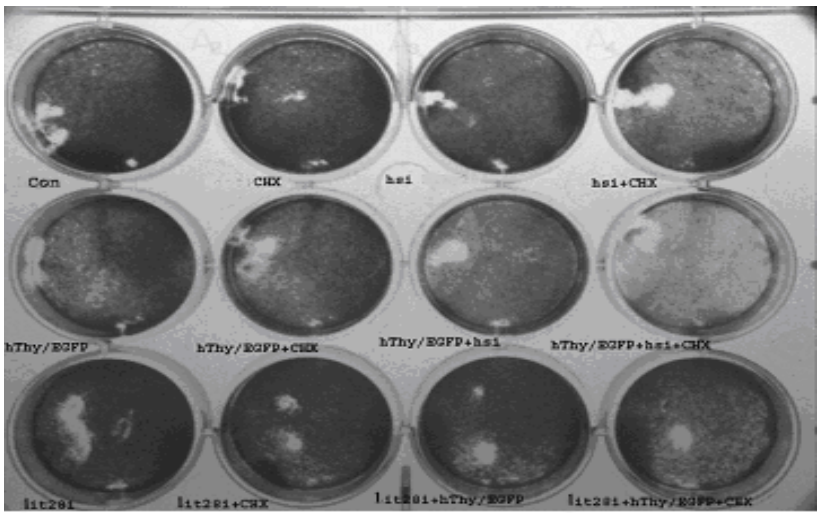

B

Densitometric Analysis of Crystal Violet Cell Staining

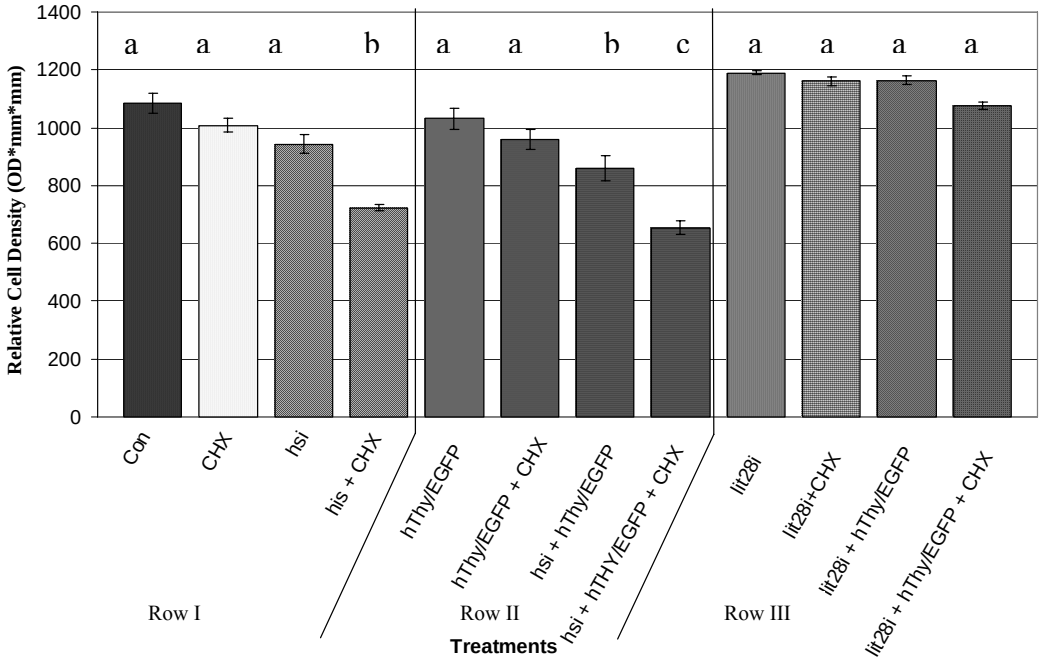

Figure 15: Crystal Violet Staining of Treated HeLa Cells. Panel A: HeLa cells were transfected with the hThy28/EGFP construct and treated with cycloheximide and/or hThy28-hsiRNA or Lit28i hsiRNA. Row I (from left to right): Control (Con), 10mM cycloheximide (CHX), 30ng/ml hThy28-hsiRNA (hsi), 30ng/ml hThy28-hsiRNA+10mM cycloheximide (hsi+CHX). Row II: 1ug/ml hThy28/EGFP plasmid DNA, 1ug/ml hThy28/EGFP+10mM cycloheximide, 1ug/ml hThy28/EGFP+30ng/ml hThy28-hsiRNA, 1ug/ml hThy28/EGFP+30ng/ml hThy28-hsiRNA+10mM cycloheximide. Row III: 30ng/ml Lit28i, 30ng/ml Lit28i+10mM cycloheximide, 30ng/ml Lit28i+1ug/ml hThy28/EGFP, 30ng/ml Lit28i+1ug/ml hThy28/EGFP+10mM Cycloheximide. **Panel B**: Densitometric analysis of the Crystal Violet stained HeLa cells shown above. The data represent the mean density +/- the standard deviation of the mean of triplicate samples. This experiment was replicated three times and the data were analyzed by ANOVA and significant difference ($p \leq .05$) among treatments were determined using Student-Newman-Keuls Method.

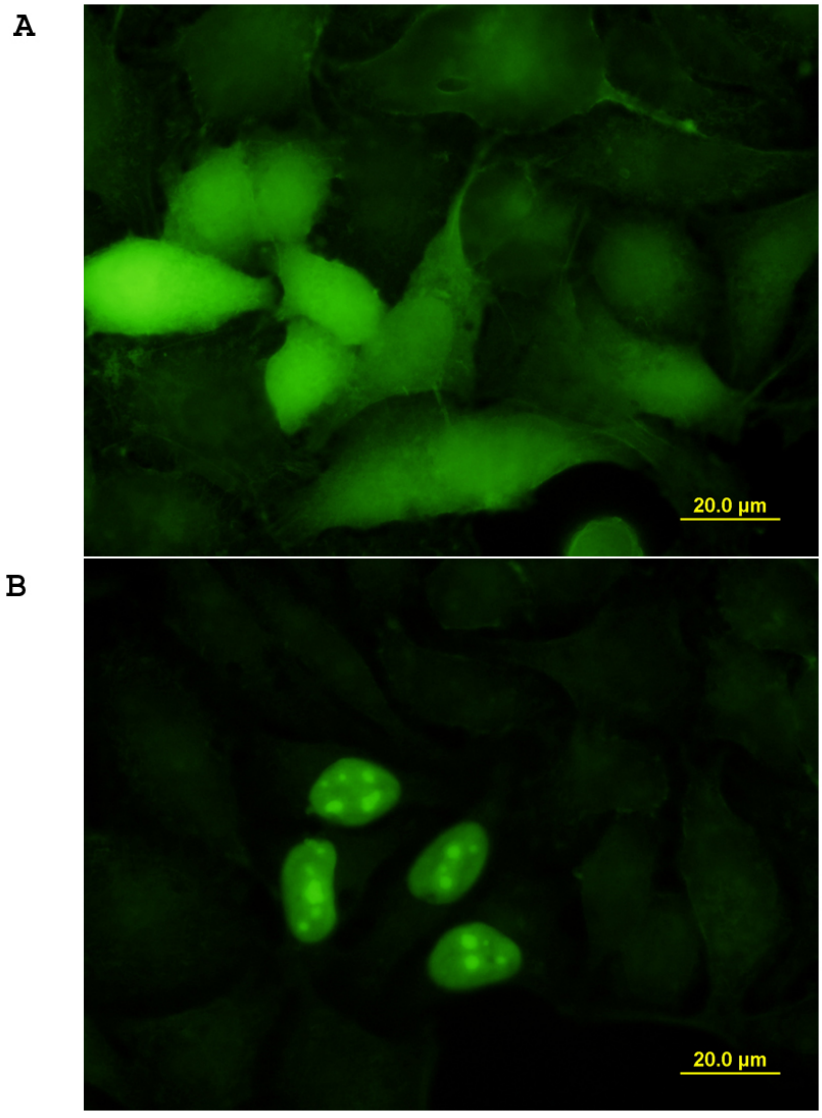

Figure 16: Nuclear Localization of the hThy28 Gene Product. The images above depict HeLa cells that were transfected with the EGFP expression plasmid and viewed under fluorescent microscopy. Panel A- HeLa cells were transfected with the EGFP expression that lacked the hThy28 insert. Panel B- HeLa cells were transfected with the hThy28/EGFP fusion gene construct. A 20.0 µm scale bar is indicated in the lower right corner of each panel.

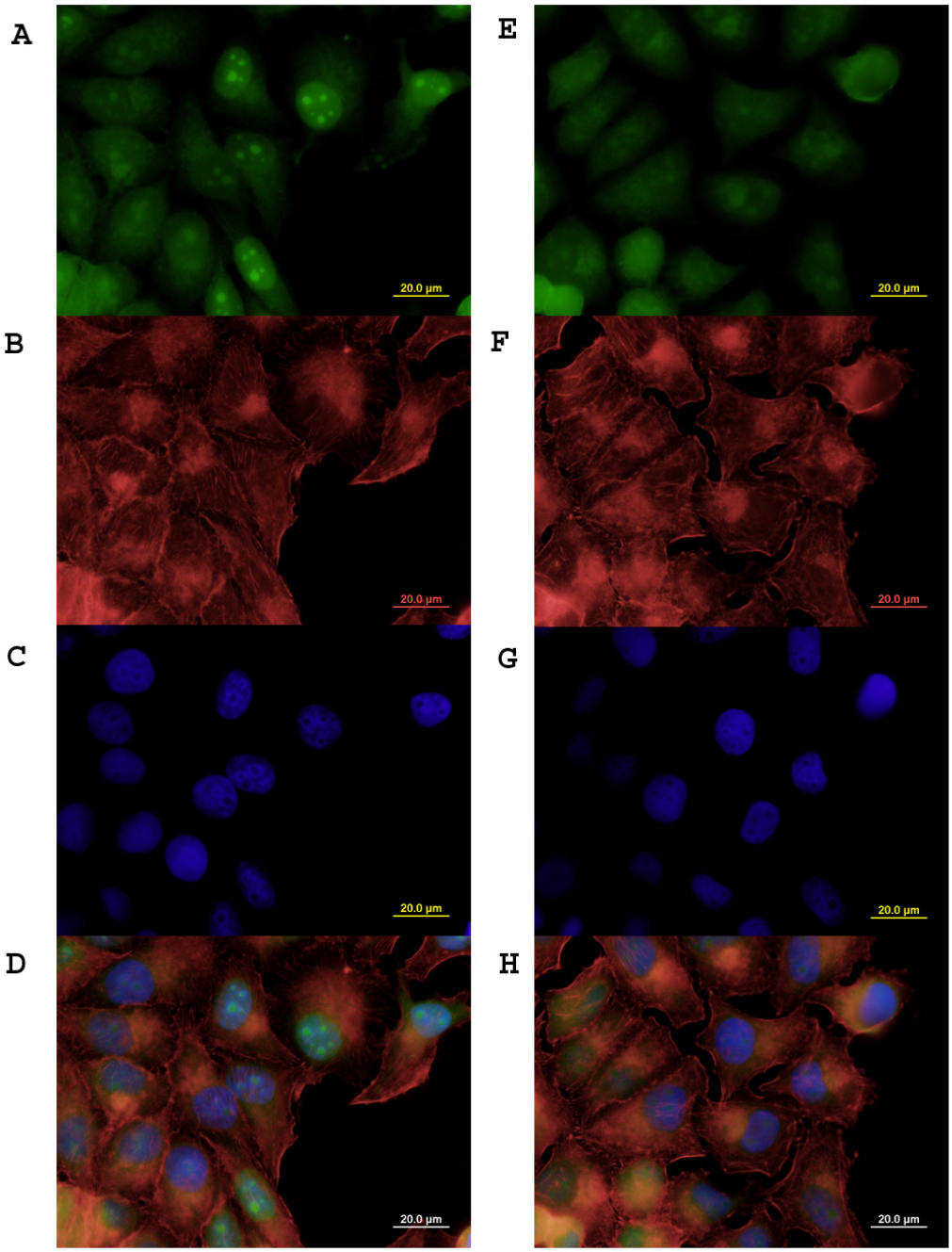

Figure 17: Nuclear Localization of hThy28 Gene Expression Showing Effects of hsiRNA. The fluorescent images above depict HeLa cells that were transfected with the hThy28/EGFP construct and viewed under fluorescent microscopy after staining with Rhodamine-labeled Phallodin and Hoescht Dye 33258. Panels A-D HeLa cells were transfected with hThy28/EGFP, alone. Panels E-H: HeLa cells transfected with hThy28/EGFP plus hThy-hsiRNA. Panels A and E demonstrate the green fluorescence of the hThy/EGFP construct. Panels B and F demonstrate the red fluorescence of Rhodamine labeled Phallodin. Panels C and G demonstrate the blue fluorescence of Hoescht Dye 33258. Panel D is a composite of Panels A-C and Panel H is a composite of Panels E-G. A 20.0 µm scale bare is indicated in the lower right corner of each panel.

A

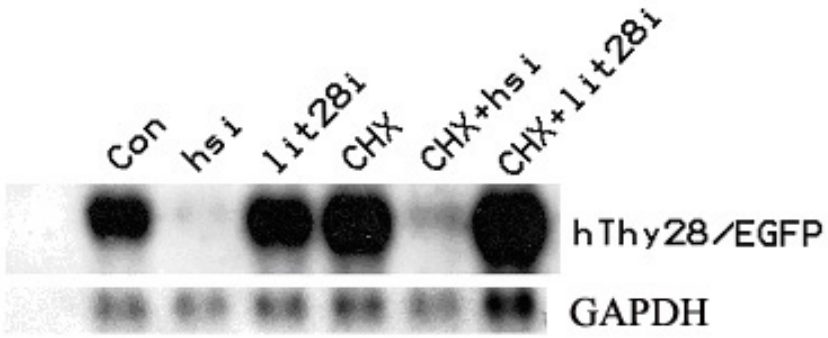

B

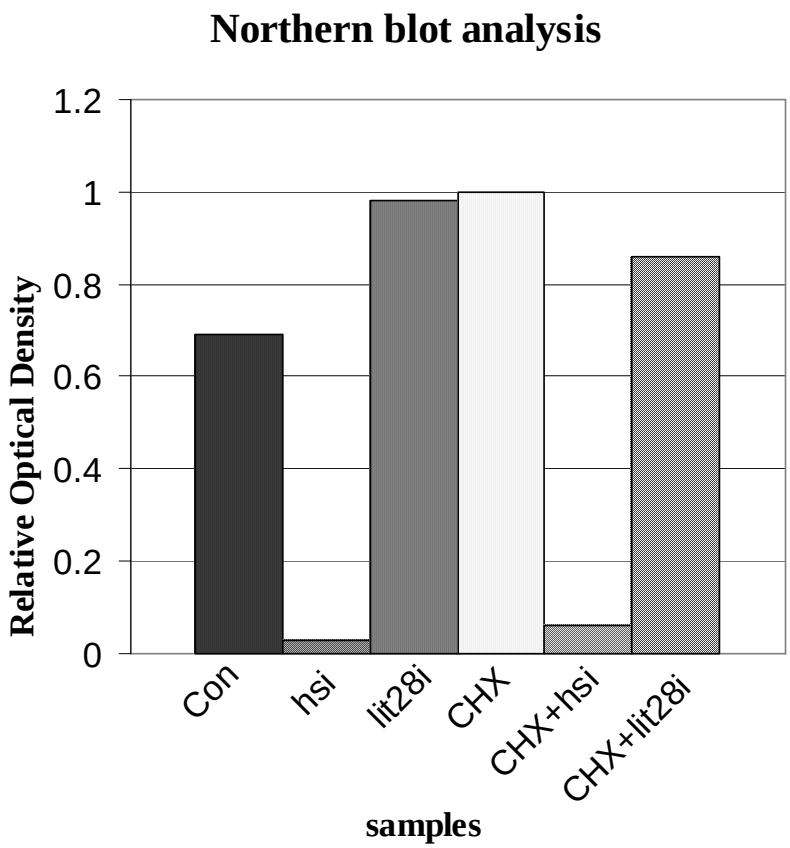

Figure 18: Northern Blot Analysis of hThy28 Expression. The figures above demonstrate the Northern Analysis performed on total RNA isolated from HeLa cells that were grown in 12 well culture plates and then transfected with the hThy28/EGFP construct; they were then treated with a control vehicle (Con), hThy-hsiRNA (hsi), the control RNAi (lit28i), cycloheximide (CHX), hThy28-hsiRNA plus cycloheximide (CHX+hsi), or the control RNAi plus cycloheximide (CHX+lit28i). Panel A is the autoradiograph demonstrating the relative level of hThy28/EGFP transcripts and GADPH transcripts. Panel B is a densitometric quantitation of the autoradiograph above demonstrating the relative level of hThy28/EGFP expression compared to GADPH.

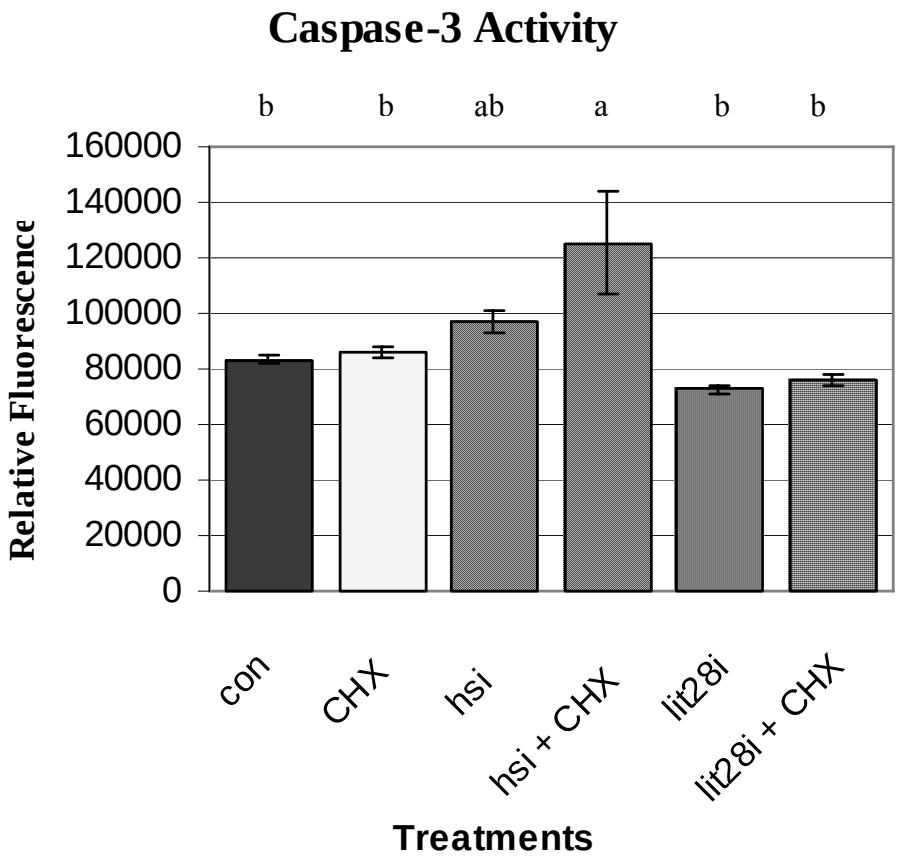

Figure 19: Caspase-3 Activity. HeLa cells were grown in 12 well culture plates and treated with a control vehicle (con), cycloheximide (CHX), hThy28-hsiRNA (hsi), hThy28-hsiRNA plus cycloheximide (hsi+CHX), control RNAi (lit28i), and control RNAi plus cyclohexamide (lit28i+CHX). Cell lysates were prepared and relative caspase activity was determined. The data above represents the relative mean fluorescence +/- the standard deviation of the mean (n=3). These data are representative of three replicated experiments.

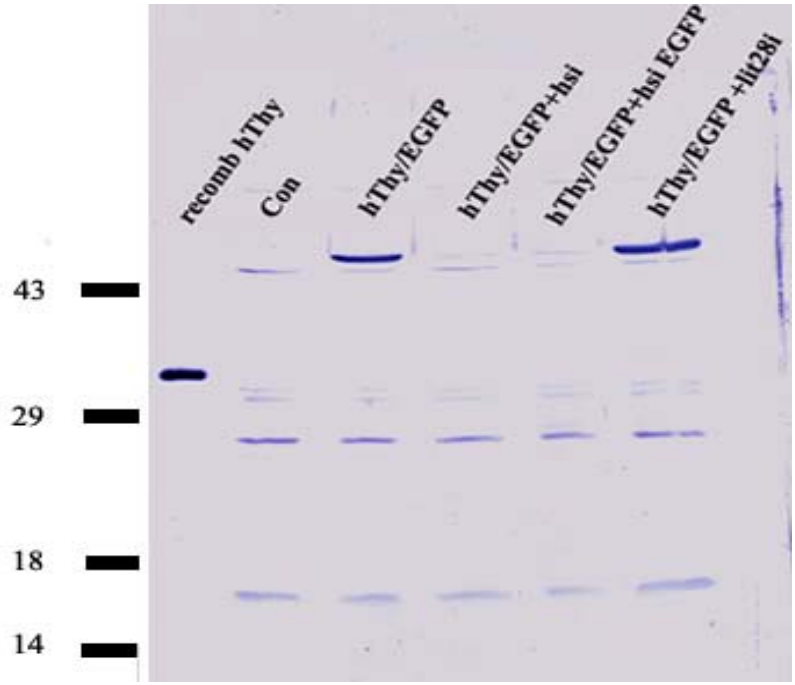

Figure 20: Western Immunoblot Analysis of Treated HeLa Cells. HeLa cells were grown in 12 well cell culture plates and treated with a control vehicle (Con), hThy28/EGFP construct (hThy/EGFP), hThy/EGFP construct plus hThy28-hsiRNA (hThy/EGFP+hsi), hThy/EGFP construct plus EGFP-hsiRNA (hThy/EGFP+hsiEGFP), or hThy/EGFP construct plus the control RNAi (hThy/EGFP+lit28i). 50ug of protein lysate from cells was electrophoretically separated on an SDS-PAG gel transferred onto PVDF membranes, and probed with anti-hThy28 antibodies. On the left, recombinant hThy28 from bacterial expression (recomb hThy) was also electrophoresed on the gel as a positive control for the anti-hThy28 antibodies. Molecular weight markers expressed in kilodaltons are indicated on the left.

CHAPTER 5

DISCUSSION

Identification of Thy28

The Thy28 gene was initially identified in avian thymocytes (cThy28)[28] using a screening procedure designed to reveal gene products that mediate avian lymphocyte apoptosis. Initial characterization of this gene, based on structural motif analysis, suggested that it encoded a nuclear localized phosphoprotein. Further examination of this gene using Northern blot analysis and Western Immunoblot analysis indicated that cThy28 is abundantly expressed in lymphoid organs and the level of this expression appears to decline in lymphocytes that are undergoing apoptosis.

The studies described herein were designed to elucidate the potential role of Thy28 in the apoptotic process. For this line of investigation, the human homologue of cThy28, HSPC144 (hThy28), was employed and apoptosis was analyzed using HeLa cells, a human carcinoma cell line. This investigative approach has several advantages. First, HeLa cells can be readily transfected at relatively high efficiencies with exogenous genes. Second, HeLa cells are large adherent cells with prominent nuclei and nucleolar structures that makes them amenable to analyzing nuclear localized proteins. Third, induction of apoptosis in HeLa cells using pharmacologic agents has been well characterized [66, 67]. And fourth, there are a wide array of commercially available antibodies directed against human apoptotic mediators that will facilitate future studies designed to delineate the apoptotic pathways that are regulated by hThy28.

Thy28 Structure

A comparison of amino acids and structural motifs of Thy28 genes in different species show high similarities in gene sequences. In comparison with other protein sequence entries in GeneBank, Thy28 has a high amino acid identity (81-96% amino acid similarity) in putative homologues among different vertebrate species (human, mouse, rat, equine, and porcine), as shown in Table 2. The number of encoded amino acids in different species is also highly conserved, for example; cThy28 contains 242 amino acids, mouse contains 226 amino acids, and HSPC144 contains 225 amino acids. Furthermore, all three of these genes are encoded by 8 exons and 7 introns. In addition, a comparison of structural motifs of different Thy28 genes shows the presence of predicted nuclear localized signals that are conserved among various species (amino acids 2-24 as shown in Figure 7). Other structural motifs including phoshorylation sites, potential glycoslysation and myristolation sites that are present in hThy28 (Figure 5) appear to be highly conserved among vertebrates (Figure 6).

Nuclear Localization of hThy28

Nuclear localization of hThy28 has been demonstrated in this study, (see Figures 16 and 17) by transfecting hThy28/EGFP constructs into HeLa cells and then observing the cells using fluorescent microscopy. The results showed that the hThy28/EGFP constructs localized to the nucleus with intense staining in the nucleolus. Subsequent treatment of cells with hThy28-hsiRNA, reduced the nucleus/nucleolar staining, confirming its nuclear location. Furthermore, in other experiments, hThy28/EGFP constructs with deleted nuclear localization signals (deletion of amino acids 3-24) failed to undergo nuclear localization when transfected into HeLa cells (Compton, personal communication).Other investigators [60] have reported the nuclear

localization of mouse Thy28 in a variety of lymphoma cell lines (WEHI-231 B cells lymphoma and mouse DO11.10 T lymphoma, human Ramos B lymphoma, and HEK293 T cells) using Western Immunoblot analysis and immunofluorescent microscopy.

The concept that hThy28 is a nucleolar protein is further supported by the inclusion of this gene (HSPC 144) in the nucleolar protein database at http://lamondlab.com/Nopdb/. This database includes over 700 nucleolar proteins,(many of which have been isolated from HeLa cells) that have been identified using high sensitivity mass spectroscopy techniques [68]. The presence of Thy28 in the nucleolus suggests that its function may be related to those of other proteins that localize to the region of the nucleus. For example, nucleolar proteins are involved in ribosomal biogenesis, RNA processing, viral replication, and tumor suppression [68, 69].

hThy28 is a Phosphoprotein

There is significant evidence that Thy28 is a phosphoprotein based on structural motif searches and immunoprecipitation experiments performend in the avian cells. Structural motif searches indicate that tyrosine kinase phosphorylation sites, as well as casein kinase II sequences are present in Thy28. Tyrosine kinase phosphorylation sites are very similar in location and amino acid identity in the mouse and human Thy28 genes based upon the sequence analysis programs such as ScanProsite (http://www.expasy.org/tools/scanprosite/) [59, 61, 70]. However, this program does not identify a tyrosine kinase phosphorylation site in cThy28, although chicken Thy28 does show a tyrosine kinase phosphorylation site according to other motif search programs (NetPhos2.0 http://www.cbs.dtu.dk/services/NetPhos/np.html) (Data not shown)[71]. Further support that Thy28 is a phosphoprotein is derived from immunoprecipitation experiment

using bursal lymphocytes and in vitro labeling with ^{32}P which clearly indicate that cThy28 is a phosphorylated protein (Compton, personal communication).

Tyrosine phosphorylation is a fundamental mechanism for many pathways that control cell growth, differentiation, and motility[72]. Thus, the presence of a tyrosine phosphorylation site in Thy28 suggests that it may play a role in these cellular processes. In addition, genes that contain casein kinase II sequences are known to be involved in cell cycle progression. The Thy28 genes of chicken, mouse, and human all have several casein kinase II phosphorylation sites in similar locations of the protein as predicted by the motif search program ScanProsite (http://www.expasy.org/tools/scanprosite/) (data not shown)[61].

DUF589 and SUMO Domains in Thy28

Two other highly conserved structural domains found in hThy28 are DUF589 and a SUMO modification sequence. Although the function of DUF589 (Domain of Undefined Function in Pfam Data Bank [73]) is unknown, the high conservation of this feature in all Thy28 genes (amino acids 54-221) suggest that it is critical to the function of this protein. Another structural motif that was identified in the hThy28 sequence was the SUMO interaction domain (AKVE at position 33-36 and MKSE at position 59-62). SUMO is an abbreviation for Small Ubiquitin-like Modifier. Sumo proteins are structurally similar to ubiquitin and they modify target proteins by covalent attachment to specific lysine residues [74]. Many of the products of SUMOylation are nuclear proteins that play important roles in regulating transcription, chromatin structure, and DNA repair [74]. Furthermore, post translational modification of proteins by SUMOylation can lead to nuclear import of the proteins, enhanced protein stability, and regulation of gene expression by SUMOylated promoter-specific transcription factors,

coactivators, or corepressors [75]. Thus, SUMOylation of Thy28 may represent a potential cellular mechanism to regulate the nuclear localization of this gene product or control its expression.

Tissue Specific Expression of Thy28

Although Thy28 was originally identified in lymphocyte cells, other studies have detected Thy28 in a variety of other organs. A Northern analysis of cThy28 expression demonstrated higher levels of transcripts in the Bursa of Fabricius, thymus, and spleen, and lower levels of expression in the liver, intestine, and heart of the chicken [28]. Conversely, in the mouse, mThy28 mRNA levels were elevated in testis, liver, brain, and kidney and lower levels in thymus, spleen, heart, and stomach in the mouse [59]. These differences in the relative levels of Thy28 mRNA in the organs of chicken and mice, could suggest that this gene may have different functions in various tissues of unrelated species.

Thy28- An Anti-Apoptotic Mediator

The studies described herein are focused on elucidating the cellular function of Thy28. As a working hypothesis, it is believed that hThy28 functions as an anti-apoptotic regulator of cell death. This premise is based on the fact that cThy28 was originally isolated in a screen for mediators of apoptosis [28]. Work from this laboratory [28] as well as others [59] has shown that a decline in Thy28 expression occurs when avian or murine lymphoid cells undergo apoptosis. Thus, in the current investigation, it was hypothesized that a reduction in hThy28 expression, using RNAi methodology, would promote cell death, when cells were stimulated to undergo apoptosis.

The crystal violet cell staining data presented in Figure 15 supports this assumption. hThy28-hsiRNA treatment exacerbated cell death when HeLa cells were stimulated to undergo apoptosis in the presence of cycloheximide. These results were further supported by the fact that caspase-3 activity (Figure 19) was significantly elevated in the presence of cycloheximide and hThy28-hsiRNA. To confirm that hThy28-hsiRNA treatment effectively reduced cellular levels of hThy28, Northern Analysis and Western Immunoblot analysis were performed; however, endogenous levels of hThy28 were below the detection limits of these assays. On the other hand, when HeLa cells were transfected with the hThy28/EGFP reporter construct, hThy28-hsiRNA clearly reduced the expression of this transfected gene, and presumably the endogenous gene, when analyzed by fluorescence microscopy (Figure 17), Northern analysis (Figure 18), and Western immunoblot analysis (Figure 20).

Heat Shock Proteins

In this study, down regulation of hThy28, combined with cycloheximide, leads to an increase in cell death (as shown in Figure 15). This increase in cell death is similar to the combined effect of silencing heat shock proteins (HSP) expression and the simultaneous exposure of cells to a genotoxic stress [76]. Heat shock proteins are a highly homologous family of chaperone proteins that oppose cell death when the cell is presented with environmental, physical, or chemical stress. HSPs protect the cells by opposing apoptotic pathways and facilitating cellular recovery [77, 78]. In studies investigating cancer cells, an elevation of heat shock proteins occurs during cell tumor genesis. This increase in HSPs correlates to an increase resistance to apoptosis [79]. One method to increase apoptosis in cancer cells is binding anti-sense oligonucleotides or short stretches of nucleic acids to homologous heat shock mRNA and

inhibiting their translation [76]. This effectively reduces the protein expression and produces the same outcome as the siRNA techniques shown in this study.

Further Directions

Clearly, further studies are required to elucidate the specific cellular function of Thy28. The data presented herein confirm that this gene product is a nuclear/nucleolar localized protein that may act as an anti-apoptotic agent. Further studies will examine how exogenous regulation of Thy28 expression (using regulatable expression vectors) affects cells undergoing apoptosis. Other studies will employ microarray analysis to examine the expression of a variety of cellular genes in response to changes in Thy28 expression. A similar microarray strategy will be employed to see if Thy28 specifically interacts with designated cellular proteins. Using this global approach to identify genes that interact with Thy28 may provide insights into cellular pathways that are regulated by expression of this gene.

REFERENCES

1. Kerr JFR, W.A., Currie AR, *Apoptosis: A Basic Biological Phenomenon with Wide-Ranging Implications in Tissue Kinetics.* British Journal of Cancer, 1972. **26**: p. 239-257.

2. Schultze-Osthoff K, F.D., Los M, Wesselborg S, Peter ME, *Apoptosis signaling by death receptors.* Eur. J. Biochem, 1998. **254**: p. 439-459.

3. Trauth BC, K.C., Peters AMJ, Siegfried M, Moller P, Falk W, Debatin K-M, Krammer P`, *Monoclonal Antibody-Mediated Tumor Regression by Induction of Apoptosis.* Science, 1989. **245**: p. 301-305.

4. Bulotta S, B.R., Rotiroti D, Borgese N, Clementi E, *Activation of the Endothelial Nitric-oxide Synthase by Tumor Necrosis Factor-a.* The Journal of Biological Chemistry, 2001. **276**(9): p. 6529-6536.

5. Fraser A, E.G., *A license to Kill.* Cell, 1996. **85**: p. 781-784.

6. Jiang XZ, T.H., Yoshimoto T, Takada E, Yoshimoto T, Kitamura T, Yamada J, Mizuguchi J, *Modulation of mThy28 nuclear protein expression during thymocyte development.* Tissue and Cell, 2003. **35**: p. 471-478.

7. Krammer, P.H., H. Kirchner, and A. Schimpl, *Lymphokines.* Immunol Today, 1989. **10**(8): p. S21-2.

8. Ekert PG, V.D., *Apoptosis and the immune system.* British Medical Bulletin, 1997. **53**(3): p. 591-603.

9. Chinnaiyan, A., Dixit VM, *The cell-death machine.* Current Biology, 1996. **6**(5): p. 555-562.

10. Osborne, C., P. Wilson, and D. Tripathy, *Oncogenes and tumor suppressor genes in breast cancer: potential diagnostic and therapeutic applications.* Oncologist, 2004. **9**(4): p. 361-77.

11. Kim, T., Kim YW, Hwang SY, Shin SM, Shin JW, Lee YH, Shin SY, Han KT, Lee JM, Namkoong SE, Kim JW, *Candidate Tumor Suppressor, HCCS-1, Is Downregulated in Human Cancers and Induces Apoptosis in Cervical Cancer.* Internation Journal of Cancer, 2002. **97**: p. 780-786.

12. Samali A, G.A., Cotter TG, *Apoptosis - the story so far...* Experientia, 1996. **52**: p. 933-941.

13. Krammer, P.H., *Lymphocyte Activation Induced Apoptosis by the APO-1 Cell Surface Receptor.* Apoptosis, Eds. E.Mihich and R.T. Schimke, Plenum Press, NY, 1994: p. 237-240.

14. Siegel RM, F.J., Zacharias DA, Chan FKM, Johnson M, Lynch D, Tsien RY, Lenardo MJ, *Fas Preassociation Required for Apoptosis Signaling and Dominant Inhibition by Pathogenic Mutations.* Science, 2000. **288**: p. 2354-2357.

15. Thorburn, A., *Death receptor-induced cell killing.* Cellular Signalling, 2004. **16**(2): p. 139-144.

16. Chun YJ, P.S., Yang AS, *Activation of Fas receptor modulates cytochrome P450 3A4 expression in human colon carcinoma cells.* Toxicology Letters, 2003. **146**(1): p. 75-81.

17. Depraetere V, G.P., *Fas and other cell death signaling pathways.* Seminars in Immunology, 1997. **9**: p. 93-107.

18. Zamzami N, S.S., Marchetti P, Hirsch T, Gomez-Monterrey I, Castedo M, Kroemer G, *Mitochondrial Control of Nuclear Apoptosis.* J.Exp. Med, 1996. **183**: p. 1533-1544.

19. Susin SA, L.H., Zamzami N, Marzo I, Brenner C, Larochette N, Prevost MC, Alzari PM, Kroemer G, *Mitochondrial Release of Caspase-2 and -9 during the Apoptotic Process.* J.Exp. Med, 1999. **189**(2): p. 381-393.

20. Sprick MR, W.H., *The interplay between the Bcl-2 family and death receptor-mediated apoptosis.* Biochimica et Biophysica Acta, 2004. **1644**: p. 125-132.

21. Budd, R.C., *Activation-induced cell death.* Current Opinion in Immunology, 2001. **12**: p. 356-362.

22. Janicke RU, E.I., Dunkern T, Kaina B, Schulze-Osthoff K, Porter AG, *Ionizing radiation but not anticancer drugs causes cell cycle arrest and failure to actiavte the mitochondrial death pathway in MCF-7 breaset carcinoma cells.* Oncogene, 2001. **20**: p. 5043-5053.

23. Silke, J., et al., *Sequence as well as functional similarity for DIABLO/Smac and Grim, Reaper and Hid?* Cell Death Differ, 2000. **7**(12): p. 1275.

24. Li P, N.D., Budihardjo I, Srinivasula SM, Ahmad M, Alnemri ES, Wang X, *Cytochrome c and dATP-Dependent Formation of Apaf-1/Caspase-9 Complex Initates an Apoptotic Protease Cascade.* Cell, 1997. **91**: p. 479-489.

25. Stennicke HR, S.G., *Caspases - controlling intracellular signals by protease zymogen activation.* Biochimica et Biophysica Acta, 2000. **1477**: p. 299-306.

26. Kerr JFR, H.B., *Definition and Incidence of Apoptosis: An Historical Perspective.* Apoptosis: The Molecular Basis of Cell Death, Cold Spring Harbor Laboratory Press, 1991: p. 5-29.

27. Wyllie, A.H., Beattie GJ, Hargreaves AD, *Chromatin changes in apoptosis.* Histochemical Journal, 1981. **13**: p. 681-692.

28. Compton MM, T.J., Icard AH, *The analysis of cThy28 expression in avian lymphocytes.* Apoptosis, 2001. **6**(4): p. 299-314.

29. Waldrip, W.R., et al., *Smad2 signaling in extraembryonic tissues determines anterior-posterior polarity of the early mouse embryo.* Cell, 1998. **92**(6): p. 797-808.

30. Compton, M.M. and J.K. Wickliffe, *Multiparametric assessment of bursal lymphocyte apoptosis.* Dev Comp Immunol, 1999. **23**(6): p. 487-500.

31. Tafani M, S.T., Pastorino JG, Farber JL, *Cytochrome c-Depenent Activation of Caspase-3 by Tumor Necrosis Factor Requires Induction of the Mitochondrial Permeability Transition.* American Journal of Pathology, 2000. **156**(6): p. 2111-2121.

32. Kwon, K.B., et al., *Molecular mechanisms of apoptosis induced by Scorpio water extract in human hepatoma HepG2 cells.* World J Gastroenterol, 2005. **11**(7): p. 943-7.

33. Nagase, M., et al., *Apoptosis induction by T-2 toxin: activation of caspase-9, caspase-3, and DFF-40/CAD through cytosolic release of cytochrome c in HL-60 cells.* Biosci Biotechnol Biochem, 2001. **65**(8): p. 1741-7.

34. Somersan, S. and N. Bhardwaj, *Tethering and tickling: a new role for the phosphatidylserine receptor.* J Cell Biol, 2001. **155**(4): p. 501-4.

35. Kietselaer, B.L., et al., *The role of labeled Annexin A5 in imaging of programmed cell death. From animal to clinical imaging.* Q J Nucl Med, 2003. **47**(4): p. 349-61.

36. Blankenberg, F., C. Mari, and H.W. Strauss, *Imaging cell death in vivo.* Q J Nucl Med, 2003. **47**(4): p. 337-48.

37. Wen, L.T., C.C. Caldwell, and A.F. Knowles, *Poly(ADP-ribose) polymerase activation and changes in Bax protein expression associated with extracellular ATP-mediated apoptosis in human embryonic kidney 293-P2X7 cells.* Mol Pharmacol, 2003. **63**(3): p. 706-13.

38. Nabha, S.M., et al., *Combretastatin-A4 prodrug induces mitotic catastrophe in chronic lymphocytic leukemia cell line independent of caspase activation and poly(ADP-ribose) polymerase cleavage.* Clin Cancer Res, 2002. **8**(8): p. 2735-41.

39. Clemons, N.J., et al., *Hsp72 inhibits Fas-mediated apoptosis upstream of the mitochondria in type II cells.* J Biol Chem, 2005. **280**(10): p. 9005-12.

40. Vanitharani R, C.P., Fauquet CM, *Short interfering RNA-mediated interference of gene expression and viral DNA accumulation in cultured plant cells.* PNAS, 2003. **100**(16): p. 9632-9636.

41. Bernstein E, D.A., Hannon GJ, *The Rest is Silence.* RNA, 2001. **7**: p. 1509-1521.

42. Napoli, C., C. Lemieux, and R. Jorgensen, *Introduction of a Chimeric Chalcone Synthase Gene into Petunia Results in Reversible Co-Suppression of Homologous Genes in trans.* Plant Cell, 1990. **2**(4): p. 279-289.

43. Carthew, R.W., *Gene Silencing by Double-Stranded RNA.* Current Opinions in Cell Biology, 2001. **13**: p. 244-248.

44. Hammond SM, C.A., Hannon GJ, *Post-Transcriptional Gene Silencing by Double-Stranded RNA.* Nature Reviews-Genetics, 2001. **2**: p. 110-119.

45. Fire, A., et al., *Potent and specific genetic interference by double-stranded RNA in Caenorhabditis elegans.* Nature, 1998. **391**(6669): p. 806-11.

46. Dong, Y. and M. Friedrich, *Nymphal RNAi: systemic RNAi mediated gene knockdown in juvenile grasshopper.* BMC Biotechnol, 2005. **5**: p. 25.

47. Ullu, E., et al., *RNA interference: advances and questions.* Philos Trans R Soc Lond B Biol Sci, 2002. **357**(1417): p. 65-70.

48. Li, H.W. and S.W. Ding, *Antiviral silencing in animals.* FEBS Lett, 2005. **579**(26): p. 5965-73.

49. Cheng JC, M.T., Sakamoto KM, *RNA Interference and Human Disease.* Molecular Genetics and Metabolism, 2003. **80**: p. 121-128.

50. Heidersbach, A., et al., *RNA interference in embryonic stem cells and the prospects for future therapies.* Gene Ther, 2006. **13**(6): p. 478-86.

51. Yu JY, D.S., Turner D, *RNA interference by expression of short-interfering RNAs and hairpin RNAs in mammalian cells.* PNAS, 2002. **99**(9): p. 6047-6052.

52. Dillin, A., *The specifics of small interfering RNA specificity.* PNAS, 2003. **100**(11): p. 6289-6291.

53. Holen T, A.M., Babaie E, Prydz H, *Similar behaviour of single-strand and double-strand siRNAs suggests they act through a common RNAi pathway.* Nucleic Acids Research, 2003. **31**(9): p. 2401-2407.

54. Paddison PJ, C.A., Bernstein E, Hannon GJ, Conklin DS, *Short hairpin RNAs (shRNAs) induce sequence-specific silencing in mammalian cells.* Genes and Development, 2002. **16**(8): p. 948-958.

55. Yang D, B.F., Huang Z, Goga A, Chen CY, Brodsky FM, Bishop JM, *Short RNA duplexes produced by hydrolysis with Escherichia coli RNase III mediate effective RNA interference in mammalian cells.* PNAS, 2002. **99**(15): p. 9942-9947.

56. Kawasaki H, S.E., Iyo M, Taira K, *siRNAs generated by recombinant human Dicer induce specific and significant but target site-independent gene silencing in human cells.* Nucleic Acids Research, 2003. **31**(3): p. 981-987.

57. Sherlock, G., *Analysis of large-scale gene expression data.* Brief Bioinform, 2001. **2**(4): p. 350-62.

58. Chi, J.T., et al., *Genomewide view of gene silencing by small interfering RNAs.* Proc Natl Acad Sci U S A, 2003. **100**(11): p. 6343-6.

59. Miyaji H, Y.T., Asakura H, Komanchi A, Kamiya S, Takasaki M, Mizuguchi J, *Molecular cloning and characterization of the mouse thymocyte protein gene.* Gene, 2002. **297**: p. 189-196.

60. Jiang XZ, T.H., Yoshimoto T, TAkada E, Asakura H, Mizuguchi J, *Anti-IgM-induced down-regulation of nuclear Thy28 protein expression in Ramos B lymphoma cells.* Apoptosis, 2003. **8**(5): p. 509-519.

61. Gattiker A, G.E., Bairoch A, *ScanProsite: a reference implementation of a PROSITE scanning tool.* Applied Bioinformatics, 2002. **1**(2): p. 107-108.

62. Park KJ, K.M., *Prediction of Nuclear Localization Signals by HMM.* http://www.jsbi.org/journal/giw99/giw99p21.pdf

63. Chenna, R., Sugawana, Hideaki, Koike, Tadashi, Lopex, Rodrigo, Gibson, Toby J, Higgens, Desmond G, Thompson, Julie D., *Multiple sequence alignment with the clustal series of programs.* Nucleic acids Res, 2003. **31**(13): p. 3497-3500.

64. Lowry, O.H., et al., *Protein measurement with the Folin phenol reagent.* J Biol Chem, 1951. **193**(1): p. 265-75.

65. Davis, A.J. and P.A. Johnson, *Expression pattern of messenger ribonucleic acid for follistatin and the inhibin/activin subunits during follicular and testicular development in gallus domesticus.* Biol Reprod, 1998. **59**(2): p. 271-7.

66. Pajak, B., B. Gajkowska, and A. Orzechowski, *Cycloheximide-mediated sensitization to TNF-alpha-induced apoptosis in human colorectal cancer cell line COLO 205; role of FLIP and metabolic inhibitors.* J Physiol Pharmacol, 2005. **56 Suppl 3**: p. 101-18.

67. Bergeron, S., M. Beauchemin, and R. Bertrand, *Camptothecin- and etoposide-induced apoptosis in human leukemia cells is independent of cell death receptor-3 and -4 aggregation but accelerates tumor necrosis factor-related apoptosis-inducing ligand-mediated cell death.* Mol Cancer Ther, 2004. **3**(12): p. 1659-69.

68. Leung, A.K., et al., *Bioinformatic analysis of the nucleolus.* Biochem J, 2003. **376**(Pt 3): p. 553-69.

69. Lam, Y.W., L. Trinkle-Mulcahy, and A.I. Lamond, *The nucleolus.* J Cell Sci, 2005. **118**(Pt 7): p. 1335-7.

70. Hulo, N., et al., *The PROSITE database.* Nucleic Acids Res, 2006. **34**(Database issue): p. D227-30.

71. Blom, N., S. Gammeltoft, and S. Brunak, *Sequence and structure-based prediction of eukaryotic protein phosphorylation sites.* J Mol Biol, 1999. **294**(5): p. 1351-62.

72. Hunter, T., *Protein kinases and phosphatases: the yin and yang of protein phosphorylation and signaling.* Cell, 1995. **80**(2): p. 225-36.

73. Song, A.X., et al., *Identification, expression, and purification of a unique stable domain from human HSPC144 protein.* Protein Expr Purif, 2005. **42**(1): p. 146-52.

74. Hilgarth, R.S., et al., *Regulation and function of SUMO modification.* J Biol Chem, 2004. **279**(52): p. 53899-902.

75. Rosendorff, A., et al., *NXP-2 association with SUMO-2 depends on lysines required for transcriptional repression.* Proc Natl Acad Sci U S A, 2006. **103**(14): p. 5308-13.

76. Zhao, Z.G. and W.L. Shen, *Heat shock protein 70 antisense oligonucleotide inhibits cell growth and induces apoptosis in human gastric cancer cell line SGC-7901.* World J Gastroenterol, 2005. **11**(1): p. 73-8.

77. Beere, H.M., *Death versus survival: functional interaction between the apoptotic and stress-inducible heat shock protein pathways.* J Clin Invest, 2005. **115**(10): p. 2633-9.

78. Beere, H.M., *"The stress of dying": the role of heat shock proteins in the regulation of apoptosis.* J Cell Sci, 2004. **117**(Pt 13): p. 2641-51.

79. Barker, C.R., et al., *Inhibition of Hsp90 acts synergistically with topoisomerase II poisons to increase the apoptotic killing of cells due to an increase in topoisomerase II mediated DNA damage.* Nucleic Acids Res, 2006. **34**(4): p. 1148-57.